Stem Cell Reports
Article

ISSCR

OPEN ACCESS

CD59 Regulation by SOX2 Is Required for Epithelial Cancer Stem Cells to Evade Complement Surveillance

Jianfeng Chen,[1] Peipei Ding,[1] Ling Li,[1] Hongyu Gu,[1] Xin Zhang,[1] Long Zhang,[1] Na Wang,[1] Lu Gan,[1] Qi Wang,[1] Wei Zhang,[1] and Weiguo Hu[1,2,*]

[1]Fudan University Shanghai Cancer Center and Institutes of Biomedical Sciences, Collaborative Innovation Center of Cancer Medicine, Shanghai Medical College, Fudan University, 270 Dong'an Road, Shanghai 200032, China

[2]Department of Immunology, Shanghai Medical College, Fudan University, 130 Dong'an Road, Shanghai 200032, China

*Correspondence: weiguohu@fudan.edu.cn

http://dx.doi.org/10.1016/j.stemcr.2016.11.008

SUMMARY

Cancer stem cells (CSCs) are highly associated with therapy resistance and metastasis. Interplay between CSCs and various immune components is required for tumor survival. However, the response of CSCs to complement surveillance remains unknown. Herein, using stem-like sphere-forming cells prepared from a mammary tumor and a lung adenocarcinoma cell line, we found that CD59 was upregulated to protect CSCs from complement-dependent cytotoxicity. *CD59* silencing significantly enhanced complement destruction and completely suppressed tumorigenesis in CSC-xenografted nude mice. Furthermore, we identified that SOX2 upregulates CD59 in epithelial CSCs. In addition, we revealed that SOX2 regulates the transcription of *mCd59b*, leading to selective mCD59b abundance in murine testis spermatogonial stem cells. Therefore, we demonstrated that CD59 regulation by SOX2 is required for stem cell evasion of complement surveillance. This finding highlights the importance of complement surveillance in eliminating CSCs and may suggest CD59 as a potential target for cancer therapy.

INTRODUCTION

Cancer stem cells (CSCs) generally account for a rare subpopulation of cells within tumors; however, some reports showed that up to 25% of cancer cells within certain tumors display the characteristics of CSCs (Kelly et al., 2007; Quintana et al., 2008). CSCs have been defined according to their ability to drive tumor growth in xenografted animals accompanied by self-renewal and differentiation (Clarke et al., 2006). Moreover, CSCs have been reported to be highly associated with therapy resistance, recurrence, and metastasis (Dean et al., 2005; Meacham and Morrison, 2013). During the process of tumor initiation and progression, tumor cells must escape immunologic detection and elimination (Dunn et al., 2002). Given these unique properties of CSCs, these cells may have a stronger capability than differentiated tumor cells of evading various host immune surveillance mechanisms.

The complement system, a main component of innate immunity, circulates to conduct immune surveillance and discriminate invading pathogens and cell debris from healthy host tissues (Morgan et al., 2005; Ricklin et al., 2010). After activation, complement components are cleaved into different fragments with multiple functions: C3a/C5a primes inflammation, C3b/iC3b induces opsono-phagocytosis, and C5b-9(n) (membrane attack complex, MAC) provokes rapid cell death (Dunkelberger and Song, 2010). To protect host cells from bystander complement attack, several membrane complement regulatory proteins (mCRPs) have evolved to restrict complement activation at diverse stages. CD46 acts as a cofactor for the inactivation of cell-bound C4b and C3b by serum factor I, CD55 inactivates C3 and C5 convertases by accelerating the decay of these proteases, and CD59 is the sole mCRP to prevent MAC formation (Zhou et al., 2008). Various endogenous (autologous antibodies, C1q, pentraxins, ficolins, etc.) (Ricklin et al., 2010) and exogenous (therapeutic antibodies, such as rituximab for B lymphoma [Zhou et al., 2008] and cetuximab for certain solid tumors [Hsu et al., 2010]) pattern recognition molecules can substantially activate complement in tumor microenvironment, which is critical in tumor cells, especially CSCs, for eventual survival from complement-mediated elimination (Ricklin et al., 2010).

Numerous studies, including ours, have demonstrated that high expression of mCRPs, mainly CD46, CD55, and CD59, confer tumor cell resistance to antibody-based cancer therapy by preventing complement cascade amplification or MAC formation; therefore, functional inhibition of mCRPs may unleash the resistance (Goswami et al., 2016; Hu et al., 2011; Macor et al., 2015; Wang et al., 2010). Compared with other mCRPs, CD59 has been considered the most effective mCRP to protect tumor cells from complement-mediated lysis (Fishelson, 2003; Zhou et al., 2008). However, there are few reports on CSC evasion of complement-mediated elimination. In addition, normal stem cells may similarly encounter frequent complement attack, which requires high expression of mCRPs. Therefore, *mCd59b* (Genbank: NM_181858.1) deficiency, but not *mCd59a* (Genbank: NM_001111060.2) deficiency, could induce male infertility associated with fewer sperm cells (Qin et al., 2003). However, the underlying

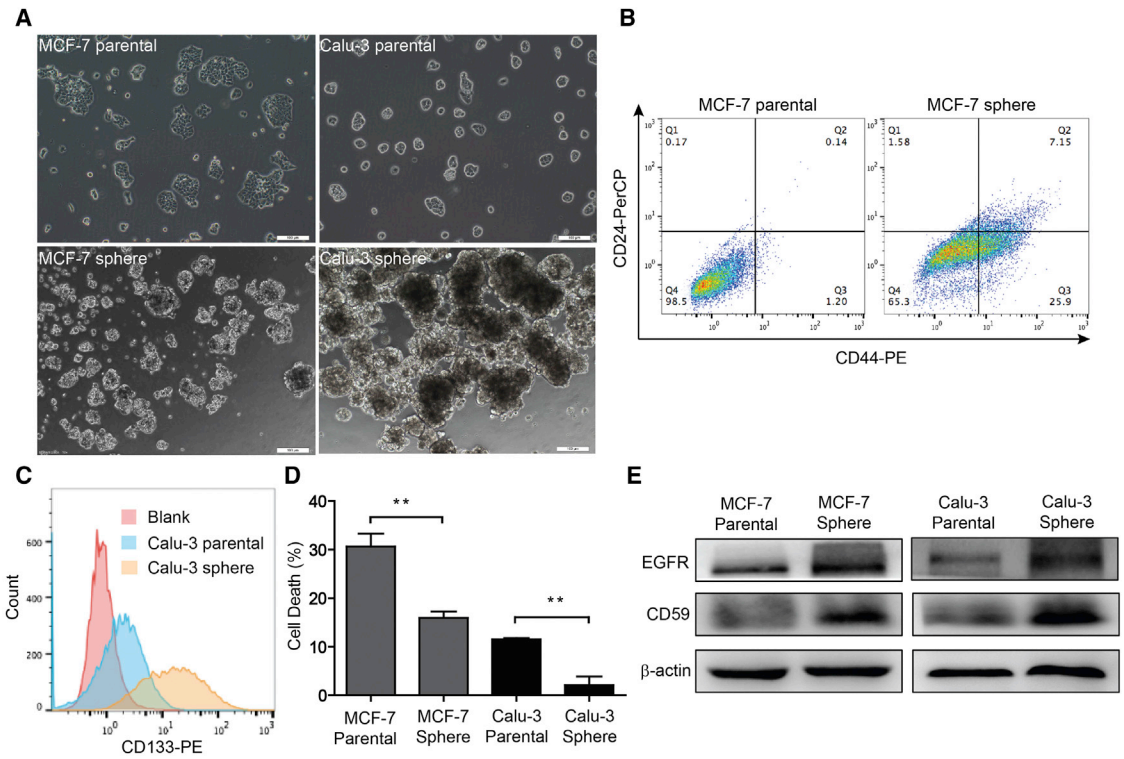

Figure 1. CD59 Upregulation Confers Stem-like Sphere-Forming Cell Resistance to Cetuximab-Induced Complement Destruction

(A) The morphological change between parental and sphere-forming cells. Scale bars, 100 μm.

(B and C) The subpopulation of stem cells was remarkably increased in the sphere-forming cells. Stem cell biomarkers: $CD44^{+}/CD24^{-}$ for MCF-7 (B) and $CD133^{+}$ for Calu-3 (C).

(D) MCF-7 and Calu-3 sphere-forming cells exhibit resistance to cetuximab-induced complement-mediated destruction compared with the parental cells. Data are presented as mean ± SD (n = 3 independent experiments); **p < 0.01.

(E) The expression levels of EGFR and CD59 were notably increased in the sphere-forming cells.

See also Figure S2.

mechanisms for stem cells escaping complement surveillance remain largely unclear.

In this study, we employed serum-free selection medium to prepare cancer stem-like sphere-forming cells in which CD59, but not CD46 or CD55, was upregulated, conferring resistance to cetuximab-induced complement-dependent cytotoxicity (CDC). CD59 insufficiency in sphere-forming cells completely suppressed tumorigenesis in xenografted nude mice. Furthermore, we illustrated that SOX2 is responsible for CD59 upregulation in CSCs and highly correlates with the selective expression of mCD59b in mouse spermatogonial stem cells.

RESULTS

CD59 Alone Is Upregulated to Confer CSC Resistance to Complement-Mediated Destruction

To investigate the response of mCRPs in CSCs, we first prepared stem-like sphere-forming cells from MCF-7 and Calu-3 parental cells. We observed that spheres developed with a diameter larger than 50 μm after 14 days of culture (Figure 1A). Furthermore, we verified the stemness of sphere-forming cells by staining the related biomarkers and by detecting in vivo tumorigenesis abilities. In MCF-7 cells, the subpopulation of stem-like $CD44^{+}/CD24^{-}$ cells was significantly increased from 1.2% in parental cells to 25.9% in sphere-forming cells (Figure 1B). Similarly, in Calu-3 sphere-forming cells, the subpopulation of $CD133^{+}$ cells was dramatically increased compared with that of the parental cells (Figure 1C). In addition, we implanted 1.0×10^{5} Calu-3 sphere and parental cells in each flank of the same nude mouse, and found that sphere-forming cells resulted in much faster tumor growth than parental cells (Figure S1). Therefore, the enriched sphere-forming cells displayed the important characteristics of CSCs.

Next, using a fluorescence-activated cell sorting (FACS) assay, we detected the expression levels of three mCRPs, CD46, CD55, and CD59, in the sphere-forming cell membranes. Compared with the parental cells, sphere-forming

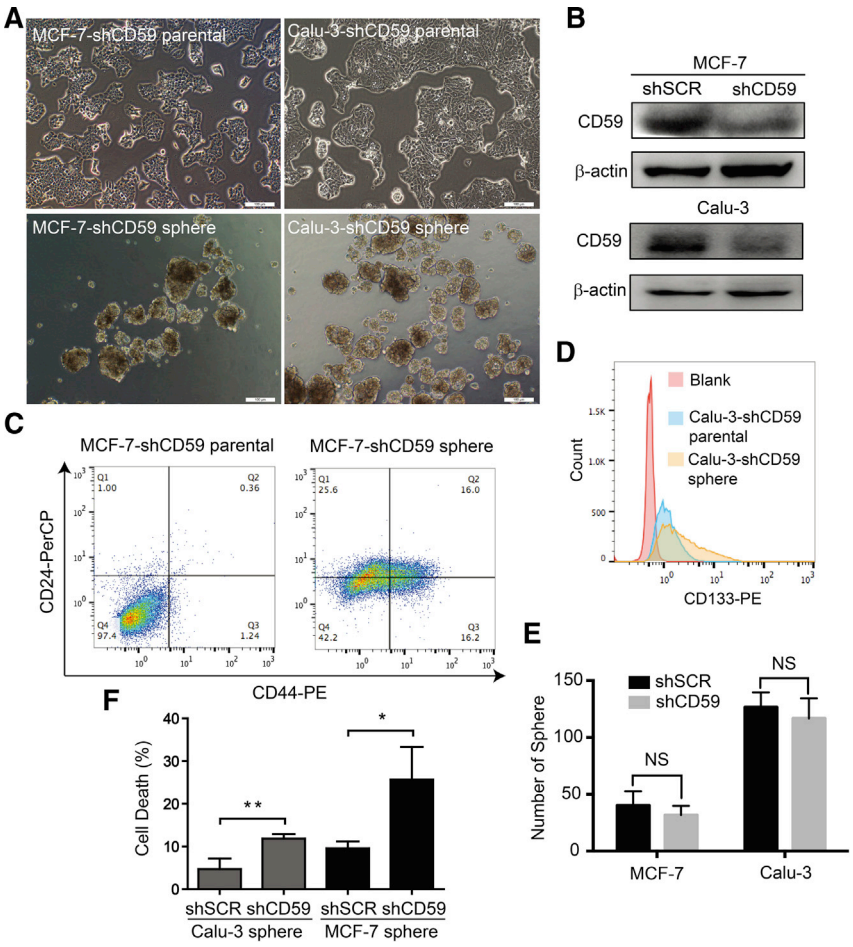

Figure 2. *CD59* Silencing Did Not Affect Sphere Formation but Sensitized Sphere-Forming Cells to Complement-Mediated Destruction

(A) *CD59* silencing in MCF-7 and Calu-3 parental cells did not affect sphere formation. Scale bars, 100 μm.

(B) Confirmation of the efficacy of *CD59* silencing. shSCR, scrambled shRNA; shCD59, specific shRNA against CD59.

(C and D) The subpopulation of stem cells was still remarkably increased in the *CD59*-silencing sphere-forming cells. Stem cell biomarkers: $CD44^{+}/CD24^{-}$ for MCF-7 (C) and $CD133^{+}$ for Calu-3 (D).

(E) Quantitative comparison of the sphere formation capacity between CD59-sufficient and CD59-insufficient cells.

(F) CD59-insufficient MCF-7 and Calu-3 sphere-forming cells were significantly vulnerable to cetuximab-induced complement destruction compared with CD59-sufficient sphere-forming cells. Data are presented as mean ± SD (n = 3 independent experiments), NS, no significance; *p < 0.05, **p < 0.01.

See also Figure S3.

cells expressed a much higher level of CD59 in both MCF-7 and Calu-3 cells (Figures S2A and S2B). In contrast, we found that the CD46 levels were significantly reduced in MCF-7 and Calu-3 sphere-forming cells, and the CD55 level was only notably reduced in MCF-7 sphere-forming cells and slightly increased in Calu-3 sphere-forming cells (Figures S2C–S2F). This finding is consistent with previous reports that CD59 is upregulated in colorectal and pancreatic CSCs (Gemei et al., 2013; Zhu et al., 2013). Therefore, CD59 may play a more important role than CD46 and CD55 in protecting CSCs from complement destruction.

To test the resistance to CDC imposed by upregulated CD59, we treated parental and sphere MCF-7 or Calu-3 cells with normal human serum (NHS) and the epidermal growth factor receptor (EGFR)-targeted monoclonal antibody cetuximab, which has been widely used for the treatment of multiple solid tumors (Hsu et al., 2010); we then measured the CDC effect by detecting lactate dehydrogenase (LDH) release. The rate of cell death in sphere-forming cells remarkably decreased compared with that of the parental cells (Figure 1D). To exclude the possibility that the EGFR expression level may decrease and accordingly reduce the CDC effect, we further detected the expression levels of EGFR accompanied by CD59 using an immunoblotting assay. We observed that the EGFR level slightly increased in both MCF-7 and Calu-3 sphere-forming cells compared with that of the parental cells (Figure 1E), which may conversely enhance the cetuximab-mediated CDC effect. Consistent with our other findings, the CD59 level still showed remarkable increases in both sphere-forming cells (Figure 1E). Together, these findings strongly suggest that CD59, but not other mCRPs, was significantly upregulated in sphere-forming CSCs to prevent complement destruction.

CD59 Insufficiency Facilitates Cetuximab-Mediated Complement Damage in CSCs

To further validate the function of CD59 in protecting CSCs from complement attack, we first generated stable CD59-insufficient MCF-7 and Calu-3 parental cells by specific small hairpin RNA (shRNA). Then, using the same method previously described, we successfully obtained sphere-forming cells after 14 days of culture (Figure 2A), and CD59 insufficiency was verified by an immunoblotting

assay (Figure 2B). Similarly, these sphere-forming cells demonstrated stemness by the significantly increased $CD44^+/CD24^-$ population in MCF-7-shCD59 sphere-forming cells and $CD133^+$ population in Calu-3-shCD59 sphere-forming cells (Figures 2C and 2D). In addition, we quantitatively compared the sphere formation capacity between CD59-sufficient and CD59-insuficient MCF-7 and Calu-3 cells, which showed no significant change (Figure 2E). Therefore, CD59 insufficiency may not affect sphere formation.

Next, we detected the ability of CD59-insufficient sphere-forming cells to avoid cetuximab-mediated CDC. As shown in Figure 2F, CD59 insufficiency resulted in the sphere-forming cells being more vulnerable to the transient cetuximab-mediated complement damage than MCF-7 and Calu-3 cells treated with scrambled shRNA. Therefore, the expression of CD59 is important for CSC survival from complement destruction.

CD59 Level Is a Determinant for the Susceptibility of Parental Cells to Complement Destruction

Considering that the implanted sphere-forming cells could sustain differentiation in in vivo experiments, we first detected the expression levels of CD59 together with CD46 and CD55 in two breast (MCF-7 and SK-BR-3) and two lung (Calu-3 and A549) parental cancer cell lines by FACS assay. As shown in Figure S3A, the CD59 level was gradually increased in the order MCF-7, SK-BR-3, A549, and Calu-3 cells. However, CD46 was expressed at the lowest level in A549 cells compared with those of MCF-7, SK-BR-3, and Calu-3 cells, which express CD46 at a similar level (Figure S3B). Moreover, we observed a notable difference in CD55 expression levels among the four cell lines in the escalating order A549, SK-BR-3, Calu-3, and MCF-7 cells, which was different from CD59 levels (Figure S3C). We also validated the mRNA and protein levels of CD59 among the four cells by qRT-PCR or western blot, respectively (Figures S3D and S3E), and the results were consistent with those in Figure S3A. Furthermore, we used cetuximab together with NHS to induce CDC in these cancer cells. The results of the LDH release assay suggested that the rate of cell death was almost exactly conversely correlated with the expression level of CD59, but not CD46 or CD55 (Figure S3F).

To further validate the role of CD59 in protecting cancer cells from cetuximab-induced CDC, we induced CD59 insufficiency by shCD59 in MCF-7 and Calu-3 cells and then measured cell survival. The results showed that compared with a scrambled control, shCD59 led to higher susceptibility of MCF-7 and Calu-3 cells to the transient cetuximab-mediated CDC (Figure S3G). Therefore, CD59 could more effectively protect cancer cells from cetuximab-induced complement destruction than CD46 and CD55, which is in agreement with the previous conclusion that CD59 is the most relevant mCRP in protecting tumor cells from complement-mediated lysis (Fishelson, 2003).

CD59 Insufficiency Completely Suppressed CSC Tumorigenesis In Vivo

To further confirm whether CD59 insufficiency makes CSCs more vulnerable to complement surveillance in vivo, we subcutaneously implanted CD59-sufficient and CD59-insufficient Calu-3 sphere-forming cells into the respective sides of nude mice axilla. The results showed that CD59 insufficiency nearly completely suppressed tumor growth compared with CD59 sufficiency (Figure 3A). Unlike CD59-sufficient sphere-forming cells, we observed that tumor growth of CD59-insufficient sphere-forming cells lessened on day 46 compared with day 43 (Figure 3A) and considered that combined treatment with the CD59 inhibitor ILYd4 and rituximab on Burkitt's B cell lymphoma xenografted tumors induced a high tumor-free rate (Hu et al., 2011). Therefore, to investigate the status of complement activation and cancer proliferation in tumor tissues, we euthanized mice and collected tumor tissues on day 46. At this endpoint, the tumor size and weight were much smaller in CD59-insufficient tumors than in CD59-sufficient tumors (Figures 3B and 3C). In addition, the CD59-insufficient tumors displayed extensive, strong C3d and MAC staining, whereas positive Ki-67 staining was almost negligible (2.8%) compared with that of CD59-sufficient tumors (65.6%) (Figure 3D). The results suggest extensive complement activation and subsequent MAC-mediated damage, thus almost completely suppressing the tumor growth of CD59-insufficient cells. In addition, we observed that a compartmented nascent lymphoid nodule with abundant lymphocyte accumulation developed and was actively predominant in CD59-insufficient tumor tissue (Figure 3D). Therefore, we suggest that the CD59-insufficient tumors would most likely disappear eventually. This finding strongly suggests that CD59 expression is required for CSC in vivo survival from persistent complement surveillance.

In addition, it has been reported that pathogen-associated molecular patterns, damage-associated molecular patterns, and surface proteins released from dead cells may activate complement (Ricklin and Lambris, 2013); therefore, we suggest that the extensive complement activation (right panel in Figure 3D) may be amplified by the initial cell death of CD59-insufficient cells. To recapitulate the complement activation in tumor tissues of nude mice implanted by CD59-insufficient cells, we treated MCF-7 parental cells with intermedilysin (ILY), which that can rapidly induce CD59-positive cell death via binding to human CD59 (Hu et al., 2008), following additional NHS or IHS (heat-inactivated human serum) administration. The

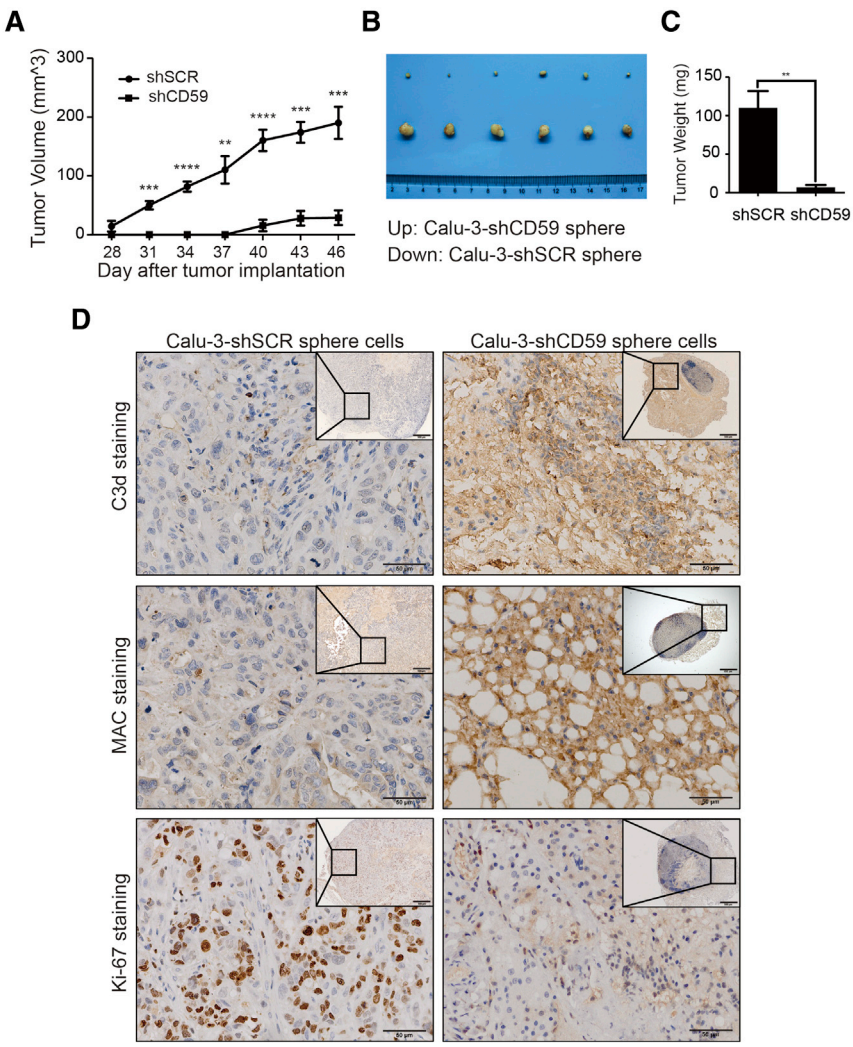

Figure 3. *CD59* Silencing Completely Suppressed Tumor Growth in Calu-3 Sphere-Forming Cells

(A) Tumor growth was completely suppressed from day 43 in nude mice implanted with CD59-insufficient Calu-3 sphere-forming cells. Data are presented as mean ± SEM (n = 6 independent experiments). The significance of tumor growth between CD59-insufficient and CD59-sufficient sphere Calu-3 cells was determined using the Holm-Sidak method in multiple t tests: one per row, with $\alpha = 5.000\%$. Each row was analyzed individually, without assuming a consistent SD. **p < 0.01, ***p < 0.001, ****p < 0.0001.

(B and C) The tumor images (B) and tumor weight (C) at the endpoint of day 46. Data are presented as mean ± SD (n = 6 independent experiments); **p < 0.01.

(D) IHC assay. Complement activation and cancer cell proliferation were determined by C3d and MAC or Ki-67 staining, respectively. Complement was substantially activated, leading to a near-complete cessation of proliferation in CD59-insufficient Calu-3 sphere-forming cells (A). Scale bar, 50 μm.

See also Figure S4.

CD59-deficient MCF-7 cells survived ILY treatment and then were positively stained by antibodies against C3d or MAC after NHS but not IHS challenge (Figures S4A and S4B). Consistent with this, complement activation triggered by NHS and ILY-induced CD59-positive dead cells resulted in higher cell death rate than ILY alone and ILY plus IHS treatment groups (Figure S4C).

SOX2 Regulates CD59 Transcription in CSCs

Our previous work illustrated that CD59 constitutive expression is regulated by Sp1, whereas nuclear factor κB (NF-κB) and CREB scaffolded by CBP/p300 proteins are responsible for the inducible expression of *CD59* (Genbank: NM_203330.2) in inflammatory conditions (Figure 5C) (Du et al., 2014). Another study showed that Smad3 also regulates *CD59* transcription in a certain condition of transforming growth factor β (TGF-β)-induced epithelial-mesenchymal transition (EMT) (Goswami et al., 2016). Therefore, to exclude the effect of the above transcription factors in regulating *CD59* transcription in CSCs, we compared their levels in nuclear extracts between the parental and sphere-forming cells. We observed that the levels of CBP/p300, phos-CREB, classic NF-κB subunits p65/p50/c-Rel, Sp1, and phos-Smad3 appear not to change or are even remarkably reduced in the sphere-forming cells (Figure 4A). These results indicate that none of these proteins contribute to CD59 upregulation in CSCs.

SOX2 is an important transcription factor that is responsible for stemness maintenance in stem cells (Malladi et al., 2016; Takahashi and Yamanaka, 2006). Using MatInspector software (Genomatix Software), we predicted a SOX2 binding site in a region from −537 to −513 bp upstream of CD59 exon 1 (Figure 4B). Therefore, we first evaluated the SOX2 level in the parental and sphere-forming cells. The results showed that SOX2 was notably upregulated in the total lysate and nuclear extract of the sphere-forming

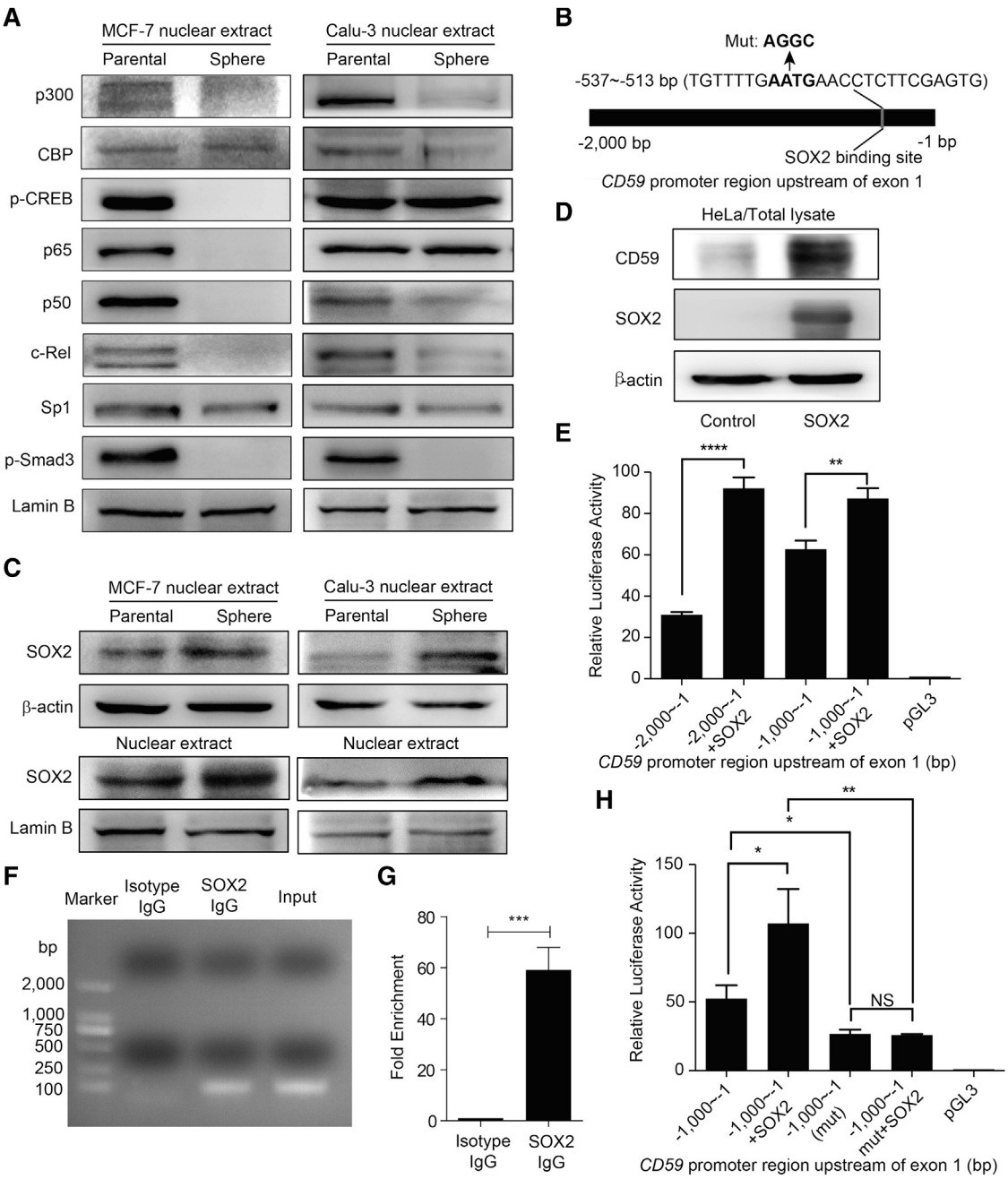

Figure 4. SOX2 Is a Key Transcription Factor for CD59 Expression in CSCs

(A) The activities or nuclear levels of reported *trans*-acting factors for *CD59* transcription were unchanged or reduced to varying degrees in stem-like sphere-forming cells.

(B) The SOX2 binding site was predicted in the region of −2,000 to −1 bp upstream of *CD59* exon1 using MatInspector software. The mutated critical response site of SOX2 is also indicated.

(C) The protein levels of SOX2 in the total lysate and nuclear extract were increased in sphere stem-like cells.

(D) Ectopic SOX2 remarkably increased CD59 expression in HeLa cells.

(E) Dual-luciferase reporter assay in HeLa cells: the promoter activities of the −2,000 to −1 bp and −1,000 to −1 bp regions upstream of *CD59* exon1 were significantly increased due to ectopic SOX2.

(F and G) ChIP assay in HeLa cells. A specific antibody against SOX2, but not isotype IgG, could capture the fragment containing the SOX2 response element in the *CD59* promoter region, which was amplified by specific primers (Table S2) using PCR (F). The quantitative data are shown (G).

(legend continued on next page)

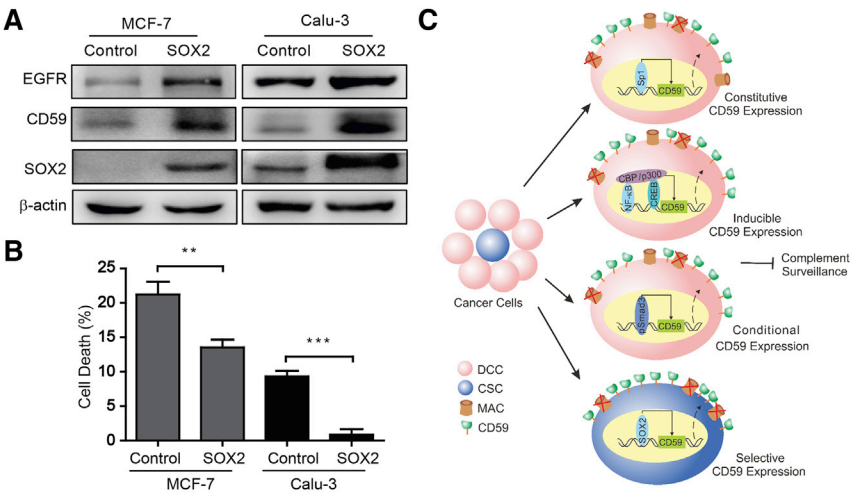

Figure 5. SOX2 Upregulates CD59 to Protect Cancer Cells from Complement Destruction

(A) Ectopic SOX2 increased the expression levels of EGFR and CD59 in parental cells.

(B) The parental cells with ectopic SOX2 were resistant to cetuximab-induced complement destruction. Data are presented as mean ± SD (n = 3 independent experiments); **p < 0.01, ***p < 0.001.

(C) Schematic for cancer cell evasion of complement surveillance by regulating *CD59* transcription. CD59 expression is constitutively regulated by Sp1, inducibly by NF-κB and CREB scaffolds bound to CBP/p300 (Du et al., 2014), conditionally by Smad3 in TGF-β-induced EMT (Goswami et al., 2016), and selectively by SOX2 in CSCs. DCC, differentiated cancer cell; CSC, cancer stem cell; MAC, membrane attack complex. See also Figure S6.

cells (Figure 4C). We then overexpressed SOX2, and found that CD59 was accordingly upregulated (Figure 4D). This observation led us to hypothesize that *CD59* transcription may be regulated by SOX2 in CSCs.

We next performed a dual-luciferase reporter assay by transfecting pGL3 plasmids containing the sequences 2,000 and 1,000 bp upstream of *CD59* exon1 alone or together with a pEGFP-N1-SOX2 plasmid into HeLa cells. The results indicate that ectopic SOX2 significantly enhanced the transcriptional activity (Figure 4E). We further identified whether SOX2 could directly bind to the predicted site by a chromatin immunoprecipitation (ChIP) assay. As shown in Figures 4F and 4G, a specific anti-SOX2 antibody, but not isotype immunoglobulin G (IgG), was able to capture the fragment that could be amplified by the specific primers for the region containing the predicted SOX2 binding site. In addition, we mutated the critical nucleotides for SOX2 activity as indicated in Figure 4B and tested the consequent promoter activity with or without ectopic SOX2. The results showed that the mutation of SOX2 response nucleotides could significantly reduce the promoter activity. Furthermore, even with ectopic SOX2, the transcriptional activity was not increased in the mutant. Mutation of the SOX2 response nucleotides completely abrogated the enhanced promoter activity by ectopic SOX2 (Figure 4H).

To further prove the regulation of *CD59* by SOX2, we constructed SOX2-insufficient stable Calu-3 and MCF7 parental cells and then generated the related stem-like sphere-forming cells. The knockdown efficiency of SOX2 was confirmed by qRT-PCR and immunoblotting (Figures S5A and S5C). We then observed that CD59 expression was accordingly downregulated in mRNA and protein levels (Figures S5B and S5C), together with the reduced protein level of EGFR (Figure S5C). Concordantly, the results of FACS further confirmed this finding and demonstrated that the expression levels of CD46 and CD55 were not influenced by SOX2 insufficiency (Figure S5D). Together, these results clearly demonstrated that SOX2 is responsible for *CD59* upregulation in CSCs.

Upregulation of CD59 by SOX2 Protects Cancer Cells from Complement Destruction

To further determine whether SOX2 is sufficient to confer cancer cell resistance to complement destruction, we overexpressed SOX2 in MCF-7 and Calu-3 cells. Using an immunoblotting assay, we found that the levels of CD59 and EGFR were increased along with ectopic SOX2 (Figure 5A). Using a FACS assay, the CD59 level in the cell membrane was further verified to be upregulated (Figures S6A and S6B), whereas the membrane levels of CD46 and CD55 did not increase compared with those of the vector control (Figures S6C–S6F).

We conducted a CDC assay to functionally test the effect of upregulated CD59 by ectopic SOX2 in protecting cancer cells from complement destruction. The results

(H) Dual-luciferase reporter assay in HeLa cells. Mutation of critical response nucleotides for SOX2 binding abrogated the enhanced promoter activity by ectopic SOX2.

Data are presented as mean ± SD (n = 3, independent repeats in E, H, and technical repeats in G). *p < 0.05, **p < 0.01, ***p < 0.001, ****p < 0.0001. See also Figure S5.

demonstrated that SOX2-overexpressing MCF-7 and Calu-3 cells are much more resistant than control cells to cetuximab-mediated complement damage (Figure 5B). These findings demonstrated that SOX2 could transcriptionally upregulate the expression of CD59, but not the expression of CD46 and CD55, in CSCs, thus conferring CSC resistance to complement surveillance (Figure 5C).

SOX2 Is Responsible for mCd59b Selective Expression in Mouse Testis

To elucidate the in vivo function of SOX2 in protecting normal stem cells from complement surveillance by upregulating CD59, we used a mouse model because of accessibility considerations. Mouse *Cd59* encodes two duplicate Cd59 isoforms, mCD59a and mCD59b (Powell et al., 1997; Qian et al., 2000). It is controversial whether the distribution of mCD59b is either universal (Qin et al., 2001) or selectively expressed in the testis (Donev et al., 2008). *mCd59b* deficiency has been reported to induce spontaneous hemolytic anemia and progressive male infertility (Qin et al., 2003). We further demonstrated the abundant expression of mCD59b in mouse testis and revealed that Sp1 regulates *mCd59a* expression widely, whereas NF-κB and serum response factor (SRF) regulate *mCd59b* transcription in inflammatory conditions to prevent complement attack (Chen et al., 2015); however, the transcriptional regulation of *mCd59b* in physiological conditions, which is helpful for explaining the abundant expression of mCD59b in mouse testis, remains unclear. Considering that SOX2 is abundant in stem cells and regulates human CD59 expression in CSCs, we propose that SOX2 may regulate *mCd59b* transcription.

Using MatInspector software, we predicted possible SOX2 response elements in the promoter regions upstream of the *mCd59a* and *mCd59b* transcriptional initiation sites. The results indicate two SOX2 binding sites locate at −153 to −124 bp upstream of *mCd59b* exon 1 (Figure 6A), whereas no SOX2 binding site is located in the *mCd59a* promoter region.

We then performed dual-luciferase reporter assays by co-transfecting pGL3 plasmid containing −350 to −1 bp region upstream of *mCd59b* exon1 and SOX2-expressing or empty vector into mouse NIH/3T3 cells. The results showed that ectopic SOX2 could dramatically enhance the promoter activity (Figure 6B). To further identify whether SOX2 directly binds to this *mCd59b* promoter region, we conducted a ChIP assay in NIH/3T3 cells that were transiently transfected by SOX2-expressing plasmid. We found that the fragment containing the SOX2 binding site, but not isotype IgG, could be remarkably enriched by specific anti-SOX2 antibody (Figures 6C and 6D). Moreover, we mutated the critical response nucleotides in two SOX2 binding sites separately or simultaneously (Figure 6A) and detected the consequent change in promoter activity. The results showed that the enhanced promoter activity almost disappeared in all three mutants with ectopic SOX2 (Figure 6E). Therefore, these results indicated that both SOX2 binding sites were essential for *mCd59b* transcription. We further functionally identified the role of SOX2 in regulating the expression of mCD59b. The results showed that the expression of mCD59b, but not mCD59a, was significantly increased (Figure 6F). Therefore, we concluded that SOX2 regulates the transcription of *mCd59b*, but not *mCd59a*.

Given the selective distribution of mCD59b in the testis (Chen et al., 2015; Donev et al., 2008), we next probed the SOX2 levels in the mouse testis, kidney, liver, colon, brain, lung, thymus, and spleen by immunohistochemistry (IHC) and found that SOX2 was exclusively enriched in testis spermatogonial stem cells compared with the other tested tissues (Figure 6G). To further identify the correlation among SOX2, mCD59a, and mCD59b during testis maturation with age, we collected the testis samples from mice aged 2, 4, 6, and 8 weeks. The result of qRT-PCR showed that compared with those in week 2, the expression levels of *mCd59a*, *mCd59b*, and *Sox2* (Genbank: NM_011443) increased, respectively, about 1.3-, 60-, and 6-fold in week 4; 2-, 110-, and 9-fold in week 6; and 2.7-, 110-, and 8-fold in week 8 (Figure S7A). We also performed RT-PCR using a pair of primers that can amplify both *mCd59a* and *mCd59b* simultaneously (Donev et al., 2008), and visualized the PCR products with 5% PAGE. As shown in Figure S7B, we found that the expression level of *mCd59a* was slightly increased, while that of *mCd59b* was dramatically increased with age. The protein levels identified by immunoblotting and IHC were also in agreement with the alteration pattern of mRNAs of *mCd59a*, *mCd59b*, and *Sox2* with age (Figures S7C and S7D). Moreover, we detected the nuclear levels of the recognized transcription factors of Sp1, SRF, canonical NF-κB, and SOX2 for *mCd59a* and *mCd59b* using an immunoblotting assay. Only SOX2 was increased with age in accordance with the alteration of mCD59b but not of mCD59a (Figure S7E). These results therefore indicate the high correlation between mCD59b and SOX2 distribution, which further supports SOX2 regulation of *mCd59b* transcription in stem cells.

DISCUSSION

CSCs account for a tiny subset of cancer cells; however, as "cancer seeds," these cells have been considered a major obstacle to curing cancer due to their characteristics of distinctive surface proteins, self-renewal, differentiation, slow-cycling state, and high association with therapy

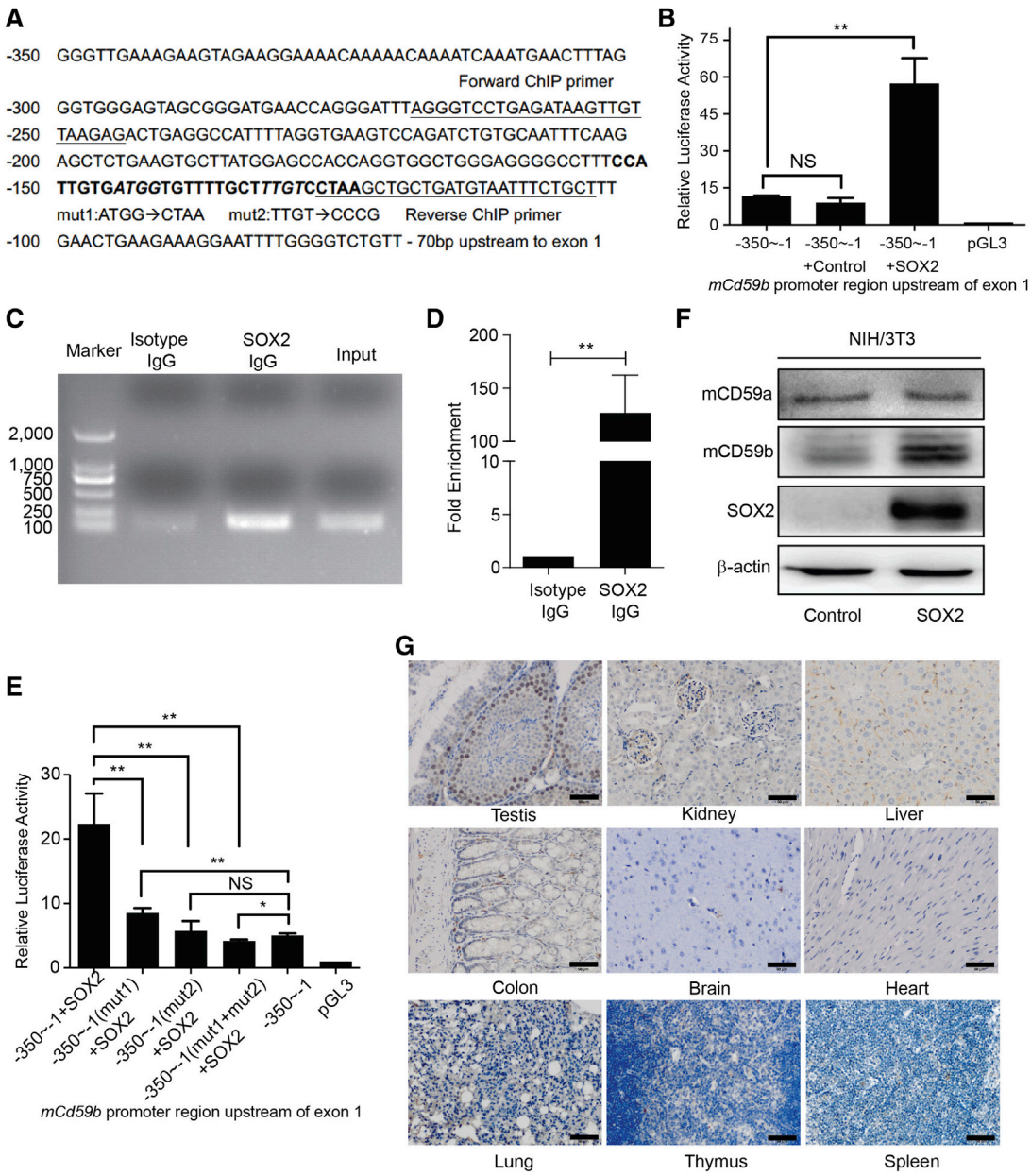

Figure 6. SOX2 Is Responsible for mCD59b-Selective Expression in Mouse Testis

(A) The sequence of the region from −350 bp to −70 bp upstream of *mCd59b* exon1, two SOX2 binding sites (bold), primer sequences, and mutated nucleotides are indicated.

(B) Dual-luciferase reporter assay in NIH/3T3 cells: ectopic SOX2 enhanced the promoter activity.

(C and D) ChIP assay in NIH/3T3 cells. A specific antibody against SOX2, but not isotype IgG, captured the fragment containing the SOX2 response element in the *mCd59b* promoter region, which was amplified by specific primers (Table S2) using PCR (C). The quantitative data are also shown (D).

(E) Dual-luciferase reporter assay in NIH/3T3 cells. Separate or simultaneous mutation of SOX2 response nucleotides in two SOX2 binding sites abrogated the enhanced promoter activity by ectopic SOX2.

(F) Ectopic SOX2 increased the expression of mCD59b, but not mCD59a, in NIH/3T3 cells.

(G) IHC assay. SOX2 is selectively abundant in testis spermatogonial stem cells, but not in the tested kidney, liver, colon, brain, heart, lung, thymus, and spleen. Scale bars, 50 μm.

Data are presented as mean ± SD (n = 3, independent repeats in B, E and technical repeat in D). NS, no significance; *$p < 0.05$, **$p < 0.01$. See also Figure S7.

resistance and metastasis (Clarke et al., 2006; Dean et al., 2005; Meacham and Morrison, 2013). Therefore, many efforts have been made to develop small molecules or antibodies that are currently in different clinical phases and that target various signaling pathways in CSCs (Kaiser, 2015). However, it is strongly suggested that CSC-specific therapy should be combined with traditional therapy to quickly eradicate whole tumors (Kaiser, 2015). Therefore, a bispecific target against differentiated and stem cancer cells may hold great potential for cancer therapy. Herein, we demonstrated that CD59 is upregulated by SOX2 in CSCs and that CD59 silencing completely eliminated tumors in a mouse model implanted with stem-like cancer cells.

Accumulating evidence has demonstrated that cancer cells are able to activate the autologous complement system (Cho et al., 2014; Fishelson, 2003; Matsumoto et al., 1997; Niculescu et al., 1992). To evade complement destruction, tumor cells upregulate mCRPs, and CD59 is the most relevant among the three mCRPs (Fishelson, 2003; Macor et al., 2015). Several reports have further shown the close relationship between CD59 expression and CSCs (Gemei et al., 2013; Zhu et al., 2013) and a high level of mCd59b, but not mCd59a, in murine spermatogonial stem cells (Donev et al., 2008). Therefore, CD59 may be such a bispecific target, and CD59-targeted therapy may significantly improve the therapeutic efficacy against cancer by simultaneously eliminating differentiated cells and CSCs, an approach that has already been suggested by several previous reports. We previously found that the human CD59-specific inhibitor ILYd4 combined with rituximab dramatically suppressed tumor growth and achieved a much higher tumor-free rate (50%) than rituximab treatment alone (8.3%) in lymphoma xenografted nude mice (Hu et al., 2011). Furthermore, the combination therapy of two bispecific antibodies against CD20 and CD55 or against CD20 and CD59 completely prevented the development of human/SCID lymphoma (Macor et al., 2015). Moreover, ectopic CD55 and/or CD59 could protect mesenchymal stem cells from complement-mediated lysis (Li and Lin, 2012).

It has been reported that SOX2 controls tumor initiation and CSC functions (Boumahdi et al., 2014); therefore, SOX2 insufficiency in glioblastoma CSCs completely suppresses proliferation and tumorigenicity (Gangemi et al., 2009). We observed that most of the signaling molecules for inducible CD59 expression, including NF-κB, CREB, CBP/p300, and Smad, were strongly inhibited (Figure 4A). This result indicates that SOX2 plays a critical role in regulating *CD59* transcription in CSCs. In addition, the normal stem cells of spermatogonia may encounter complement attack, and there is an intact complement system in the female genital tract (Harris et al., 2006); therefore, spermatozoa require the high expression of mCRPs such as CD59. The deficiency of *mCd59b* resulted in progressive male infertility due to immobile dysmorphic and fewer sperm cells (Qin et al., 2003), indicating the critical role of CD59 in protecting spermatozoa from complement attack. In this study, we further demonstrated that SOX2, which is abundant in mouse testis, is responsible for mCD59b, but not mCD59a, selective expression in mouse testis. Considering the stemness of mouse spermospore and the previous reports that *mCd59b* deficiency resulted in mouse progressive male infertility due to low sperm count and mobility (Qin et al., 2003) and mCD59b is selectively expressed in mouse testis (Chen et al., 2015; Donev et al., 2008), our finding that SOX2 regulates *mCd59b* transcription in testis may explain the importance of human CD59 expression in CSCs in protecting them from complement attack. Therefore, we conclude that the loss of tumor-initiating ability and tumorigenicity in CSCs by *SOX2* (Genbank: NM_003106) silencing resulted, at least in part, from the consequent CD59 insufficiency.

Recently, a stem-like cancer cell termed latency competent cancer cells, which express SOX2 and Sox9, have been reported to evade natural killer (NK) cell-mediated clearance by attenuating WNT signaling, thereby downregulating ligand expression for NK cell activity (Malladi et al., 2016). Herein, we interestingly observed that SOX2 also regulates EGFR expression, which may confer CSCs a growth signaling for their survival in the tumor microenvironment. Importantly, we further extend the role of SOX2 in protecting CSCs from another innate immune surveillance mechanism. SOX2 regulates CD59 expression in CSCs, and CD59 insufficiency induced a near-complete cessation of proliferation and loss of tumorigenesis in CSCs. This finding highlights the importance of complement surveillance in clearing tumor cells and suggests CD59 as a potential target in cancer therapy.

EXPERIMENTAL PROCEDURES

Sphere Formation Assay

The sphere formation assay was performed as previously described (Rybak et al., 2011; Vlashi et al., 2009). In brief, CD59-sufficient or CD59-insufficient parental cells were dissociated with 0.25% trypsin/EDTA and resuspended with a serum-free medium (DMEM/F12, 3:1 mixture) containing 0.4% BSA and 0.2× B27 lacking vitamin A and supplemented with recombinant EGF (PeproTech) at 10 ng/mL and recombinant basic fibroblast growth factor (PeproTech) at 10 ng/mL. For examination of the sphere-forming capacity of cancer cells, cells were enzymatically dissociated and resuspended at a density of 10,000 cells/mL with the above medium and plated in ultra-low attachment 24-well plates. The medium was exchanged every 7 days, and the spheres were counted and harvested at 14 days. Sphere-forming cells were

subcultured with TrypLE Express (Gibco) and resuspended in the above medium at clonal density. The sphere-forming capacity and morphology did not alter even with passage over 15 generations.

CDC Assay

The CDC assay was performed according to our previous report with minor modifications (Hu et al., 2011). In brief, 10,000 cancer cells were plated in 96-well plates for 16 hr and then treated with 200 μg/mL of cetuximab (Merck) and 20% NHS or IHS for 1.5 hr. For evaluation of the CDC effect, released LDH was measured in the supernatant using the Cytotoxicity Detection kit (Roche) based on the manufacturer's instructions. The optical density was measured at 490 nm with a Synergy HT microplate reader (Bio-Tek).

Xenograft Tumors

Six-week-old male BALB/c nude mice were purchased from Vital River. In total, two pairs of cells, 10^5 Calu-3-shSCR and Calu-3-shCD59 sphere-forming cells, or 10^5 Calu-3 sphere and parental cells were resuspended in a PBS/Matrigel (Invitrogen) mixture (1:1 volume) and then subcutaneously injected into the left or right sides of the axilla, respectively. The mice were inspected for tumor appearance, and tumor growth was measured every 3 days using a caliper. The tumor volume was determined following a standard formula: length × width^2/2. The presence of tumor was confirmed by necropsy, and all the animal experiments were conducted in accordance with experimental protocols approved by the Animal Ethics Committee at Shanghai Medical School, Fudan University.

Statistical Analysis

The data are presented as the mean ± SD unless otherwise specified. The significant differences between two groups were determined using the two-tailed Student's t test for unpaired data, and $p < 0.05$ was considered statistically significant.

SUPPLEMENTAL INFORMATION

Supplemental Information includes Supplemental Experimental Procedures, seven figures, and two tables and can be found with this article online at http://dx.doi.org/10.1016/j.stemcr.2016.11.008.

AUTHOR CONTRIBUTIONS

J.C. and W.H. designed experiments and co-wrote the manuscript. J.C. performed most experiments and analyzed the data. J.C., P.D., L.L., H.G., Q.W., and W.Z. conducted the remaining mouse experiments. X.Z., L.Z., L.G., and N.W. provided technical and material support. W.H. conceptualized and designed the project.

ACKNOWLEDGMENTS

This work was supported by grants to W.H. from the National Natural Science Foundation of China (81372258, 81572827), the Major State Basic Research Development Program of China (2013CB910802), and the Program for Professor of Special Appointment (Eastern Scholar, GZ2014002) at Shanghai Institutions of Higher Learning.

Received: May 17, 2016
Revised: November 21, 2016
Accepted: November 22, 2016
Published: December 22, 2016

REFERENCES

Boumahdi, S., Driessens, G., Lapouge, G., Rorive, S., Nassar, D., Le Mercier, M., Delatte, B., Caauwe, A., Lenglez, S., Nkusi, E., et al. (2014). SOX2 controls tumour initiation and cancer stem-cell functions in squamous-cell carcinoma. Nature *511*, 246–250.

Chen, J., Du, Y., Ding, P., Zhang, X., Zhang, L., Wang, N., and Hu, W. (2015). Mouse Cd59b but not Cd59a is upregulated to protect cells from complement attack in response to inflammatory stimulation. Genes Immun. *16*, 437–445.

Cho, M.S., Vasquez, H.G., Rupaimoole, R., Pradeep, S., Wu, S., Zand, B., Han, H.D., Rodriguez-Aguayo, C., Bottsford-Miller, J., Huang, J., et al. (2014). Autocrine effects of tumor-derived complement. Cell Rep. *6*, 1085–1095.

Clarke, M.F., Dick, J.E., Dirks, P.B., Eaves, C.J., Jamieson, C.H., Jones, D.L., Visvader, J., Weissman, I.L., and Wahl, G.M. (2006). Cancer stem cells—perspectives on current status and future directions: AACR Workshop on cancer stem cells. Cancer Res. *66*, 9339–9344.

Dean, M., Fojo, T., and Bates, S. (2005). Tumour stem cells and drug resistance. Nat. Rev. Cancer *5*, 275–284.

Donev, R.M., Sivasankar, B., Mizuno, M., and Morgan, B.P. (2008). The mouse complement regulator CD59b is significantly expressed only in testis and plays roles in sperm acrosome activation and motility. Mol. Immunol. *45*, 534–542.

Du, Y., Teng, X., Wang, N., Zhang, X., Chen, J., Ding, P., Qiao, Q., Wang, Q., Zhang, L., Yang, C., et al. (2014). NF-kappaB and enhancer-binding CREB protein scaffolded by CREB-binding protein (CBP)/p300 proteins regulate CD59 protein expression to protect cells from complement attack. J. Biol. Chem. *289*, 2711–2724.

Dunkelberger, J.R., and Song, W.C. (2010). Complement and its role in innate and adaptive immune responses. Cell Res. *20*, 34–50.

Dunn, G.P., Bruce, A.T., Ikeda, H., Old, L.J., and Schreiber, R.D. (2002). Cancer immunoediting: from immunosurveillance to tumor escape. Nat. Immunol. *3*, 991–998.

Fishelson, Z. (2003). Obstacles to cancer immunotherapy: expression of membrane complement regulatory proteins (mCRPs) in tumors. Mol. Immunol. *40*, 109–123.

Gangemi, R.M., Griffero, F., Marubbi, D., Perera, M., Capra, M.C., Malatesta, P., Ravetti, G.L., Zona, G.L., Daga, A., and Corte, G. (2009). SOX2 silencing in glioblastoma tumor-initiating cells causes stop of proliferation and loss of tumorigenicity. Stem Cells *27*, 40–48.

Gemei, M., Di Noto, R., Mirabelli, P., and Del Vecchio, L. (2013). Cytometric profiling of CD133+ cells in human colon carcinoma cell lines identifies a common core phenotype and cell type-specific mosaics. Int. J. Biol. Markers *28*, 267–273.

Goswami, M.T., Reka, A.K., Kurapati, H., Kaza, V., Chen, J., Standiford, T.J., and Keshamouni, V.G. (2016). Regulation of complement-dependent cytotoxicity by TGF-beta-induced epithelial-mesenchymal transition. Oncogene *35*, 1888–1898.

Harris, C.L., Mizuno, M., and Morgan, B.P. (2006). Complement and complement regulators in the male reproductive system. Mol. Immunol. *43*, 57–67.

Hsu, Y.F., Ajona, D., Corrales, L., Lopez-Picazo, J.M., Gurpide, A., Montuenga, L.M., and Pio, R. (2010). Complement activation mediates cetuximab inhibition of non-small cell lung cancer tumor growth in vivo. Mol. Cancer *9*, 139.

Hu, W., Ferris, S.P., Tweten, R.K., Wu, G., Radaeva, S., Gao, B., Bronson, R.T., Halperin, J.A., and Qin, X. (2008). Rapid conditional targeted ablation of cells expressing human CD59 in transgenic mice by intermedilysin. Nat. Med. *14*, 98–103.

Hu, W., Ge, X., You, T., Xu, T., Zhang, J., Wu, G., Peng, Z., Chorev, M., Aktas, B.H., Halperin, J.A., et al. (2011). Human CD59 inhibitor sensitizes rituximab-resistant lymphoma cells to complement-mediated cytolysis. Cancer Res. *71*, 2298–2307.

Kaiser, J. (2015). The cancer stem cell gamble. Science *347*, 226–229.

Kelly, P.N., Dakic, A., Adams, J.M., Nutt, S.L., and Strasser, A. (2007). Tumor growth need not be driven by rare cancer stem cells. Science *317*, 337.

Li, Y., and Lin, F. (2012). Mesenchymal stem cells are injured by complement after their contact with serum. Blood *120*, 3436–3443.

Macor, P., Secco, E., Mezzaroba, N., Zorzet, S., Durigutto, P., Gaiotto, T., De Maso, L., Biffi, S., Garrovo, C., Capolla, S., et al. (2015). Bispecific antibodies targeting tumor-associated antigens and neutralizing complement regulators increase the efficacy of antibody-based immunotherapy in mice. Leukemia *29*, 406–414.

Malladi, S., Macalinao, D.G., Jin, X., He, L., Basnet, H., Zou, Y., de Stanchina, E., and Massague, J. (2016). Metastatic latency and immune evasion through autocrine inhibition of WNT. Cell *165*, 45–60.

Matsumoto, M., Takeda, J., Inoue, N., Hara, T., Hatanaka, M., Takahashi, K., Nagasawa, S., Akedo, H., and Seya, T. (1997). A novel protein that participates in nonself discrimination of malignant cells by homologous complement. Nat. Med. *3*, 1266–1270.

Meacham, C.E., and Morrison, S.J. (2013). Tumour heterogeneity and cancer cell plasticity. Nature *501*, 328–337.

Morgan, B.P., Marchbank, K.J., Longhi, M.P., Harris, C.L., and Gallimore, A.M. (2005). Complement: central to innate immunity and bridging to adaptive responses. Immunol. Lett. *97*, 171–179.

Niculescu, F., Rus, H.G., Retegan, M., and Vlaicu, R. (1992). Persistent complement activation on tumor cells in breast cancer. Am. J. Pathol. *140*, 1039–1043.

Powell, M.B., Marchbank, K.J., Rushmere, N.K., van den Berg, C.W., and Morgan, B.P. (1997). Molecular cloning, chromosomal localization, expression, and functional characterization of the mouse analogue of human CD59. J. Immunol. *158*, 1692–1702.

Qian, Y.M., Qin, X., Miwa, T., Sun, X., Halperin, J.A., and Song, W.C. (2000). Identification and functional characterization of a new gene encoding the mouse terminal complement inhibitor CD59. J. Immunol. *165*, 2528–2534.

Qin, X., Miwa, T., Aktas, H., Gao, M., Lee, C., Qian, Y.M., Morton, C.C., Shahsafaei, A., Song, W.C., and Halperin, J.A. (2001). Genomic structure, functional comparison, and tissue distribution of mouse Cd59a and Cd59b. Mamm. Genome *12*, 582–589.

Qin, X., Krumrei, N., Grubissich, L., Dobarro, M., Aktas, H., Perez, G., and Halperin, J.A. (2003). Deficiency of the mouse complement regulatory protein mCd59b results in spontaneous hemolytic anemia with platelet activation and progressive male infertility. Immunity *18*, 217–227.

Quintana, E., Shackleton, M., Sabel, M.S., Fullen, D.R., Johnson, T.M., and Morrison, S.J. (2008). Efficient tumour formation by single human melanoma cells. Nature *456*, 593–598.

Ricklin, D., and Lambris, J.D. (2013). Complement in immune and inflammatory disorders: pathophysiological mechanisms. J. Immunol. *190*, 3831–3838.

Ricklin, D., Hajishengallis, G., Yang, K., and Lambris, J.D. (2010). Complement: a key system for immune surveillance and homeostasis. Nat. Immunol. *11*, 785–797.

Rybak, A.P., He, L., Kapoor, A., Cutz, J.C., and Tang, D. (2011). Characterization of sphere-propagating cells with stem-like properties from DU145 prostate cancer cells. Biochim. Biophys. Acta *1813*, 683–694.

Takahashi, K., and Yamanaka, S. (2006). Induction of pluripotent stem cells from mouse embryonic and adult fibroblast cultures by defined factors. Cell *126*, 663–676.

Vlashi, E., Kim, K., Lagadec, C., Donna, L.D., McDonald, J.T., Eghbali, M., Sayre, J.W., Stefani, E., McBride, W., and Pajonk, F. (2009). In vivo imaging, tracking, and targeting of cancer stem cells. J. Natl. Cancer Inst. *101*, 350–359.

Wang, H., Liu, Y., Li, Z.Y., Fan, X., Hemminki, A., and Lieber, A. (2010). A recombinant adenovirus type 35 fiber knob protein sensitizes lymphoma cells to rituximab therapy. Blood *115*, 592–600.

Zhou, X., Hu, W., and Qin, X. (2008). The role of complement in the mechanism of action of rituximab for B-cell lymphoma: implications for therapy. Oncologist *13*, 954–966.

Zhu, J., Nie, S., Wu, J., and Lubman, D.M. (2013). Target proteomic profiling of frozen pancreatic CD24+ adenocarcinoma tissues by immuno-laser capture microdissection and nano-LC–MS/MS. J. Proteome Res. *12*, 2791–2804.

Stem Cell Reports, Volume *8*

Supplemental Information

CD59 Regulation by SOX2 Is Required for Epithelial Cancer Stem Cells to Evade Complement Surveillance

Jianfeng Chen, Peipei Ding, Ling Li, Hongyu Gu, Xin Zhang, Long Zhang, Na Wang, Lu Gan, Qi Wang, Wei Zhang, and Weiguo Hu

Supporting Information

Chen et al.

Supplemental Figures and Legends

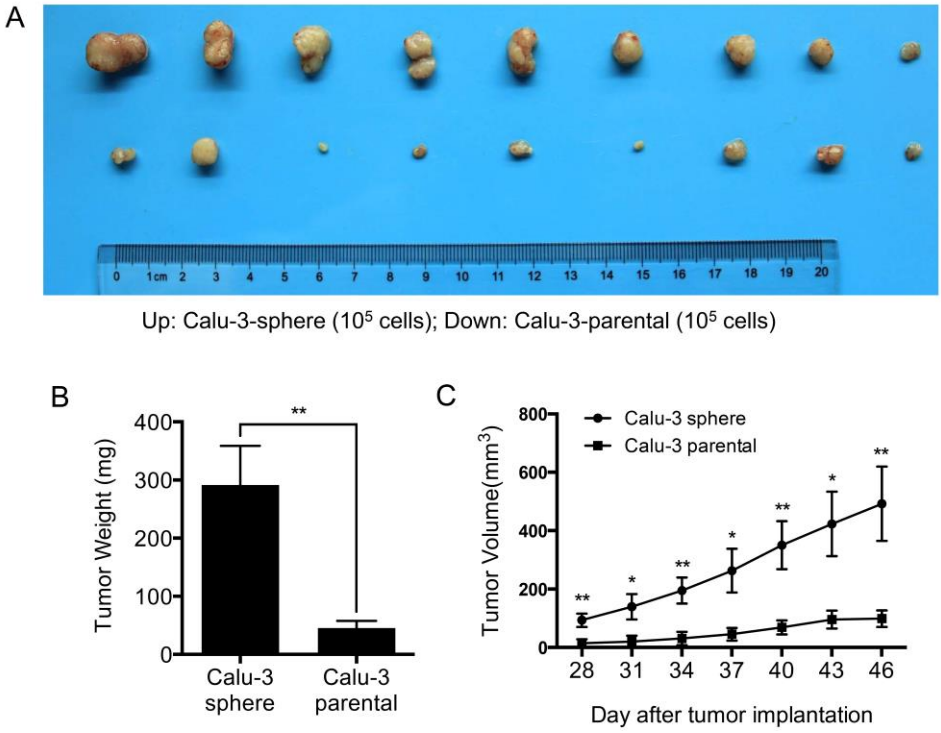

Figure S1. Stem-like Calu-3 sphere forming cells display higher tumor-initiating capability than parental cells, related to results. Same amount of sphere or parental cells were subcutaneously injected into the left or right sides of the nude mouse axilla, respectively. Tumor size was measured twice per week staring from day 28 after implantation, and the experiment was terminated at day 46. (A and B) Tumor image (A) and tumor weight (B) at the end-point of experiments. (C) Tumor growth curve. Data represent mean ± SEM (n=9, independent experiments). *, $P < 0.05$; **, $P < 0.01$.

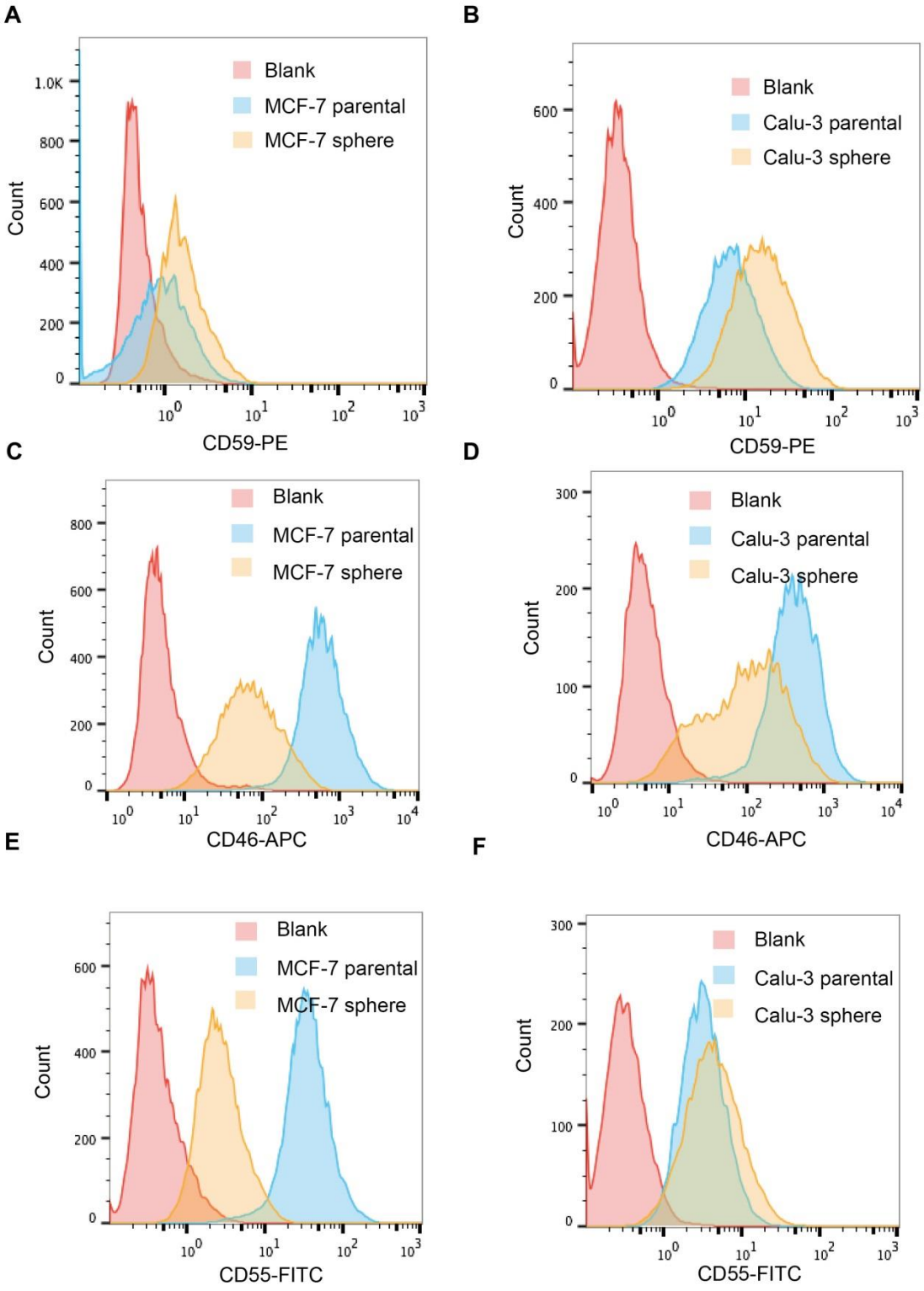

Figure S2. Comparison of the expression level changes in CD59, CD46 and CD55 between the parental and sphere cancer cells, related to Figure 1. (A and B) The CD59 levels were remarkably increased in MCF-7 (A) and

Calu-3 (B) sphere forming cells. (C and D) The CD46 levels were remarkable reduced in MCF-7 (C) and Calu-3 (D) sphere forming cells. (E and F) The CD55 levels were dramatically reduced in MCF-7 sphere forming cells (E) and slightly increased in Calu-3 sphere forming cells (F).

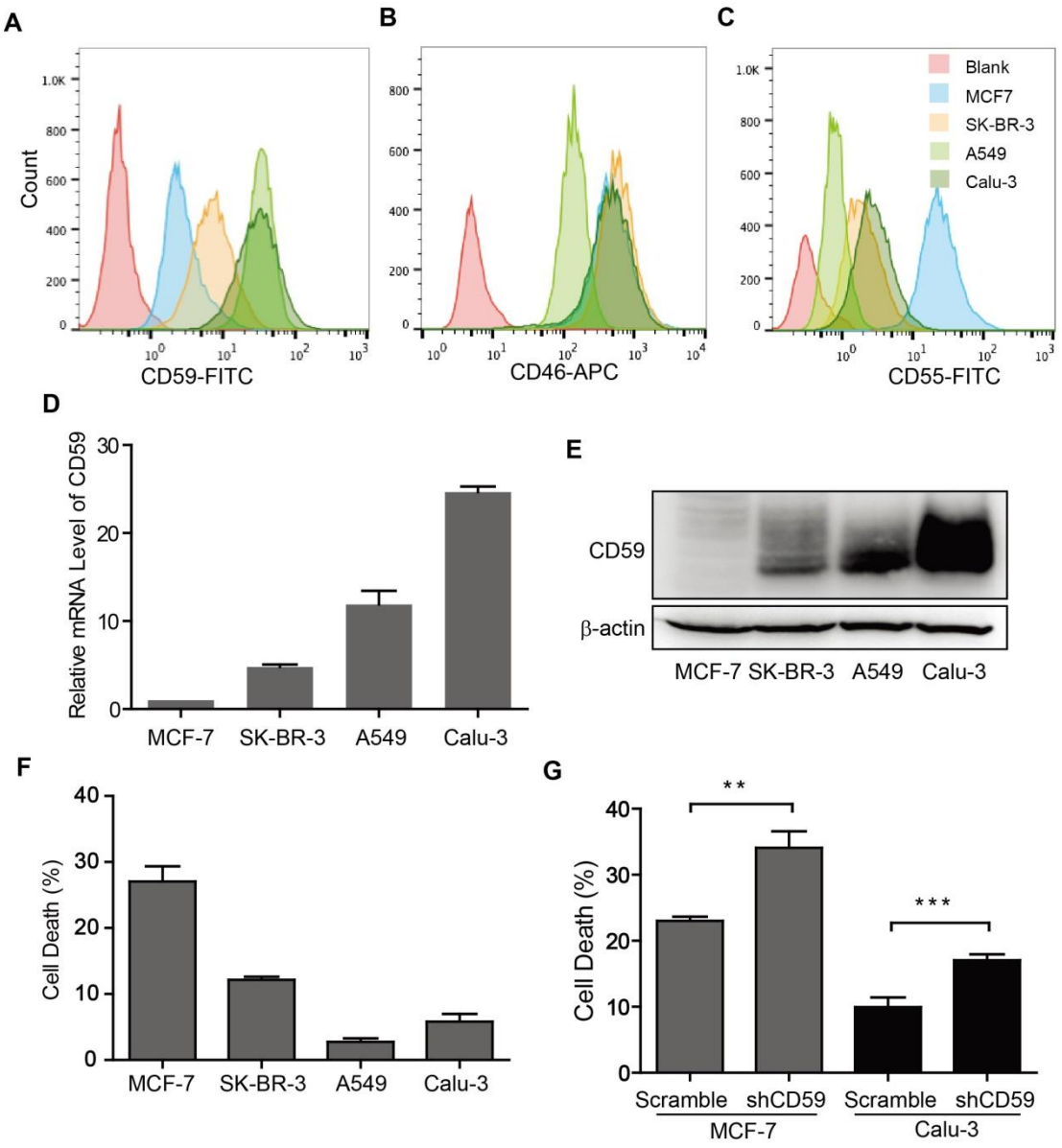

Figure S3. CD59 is the most relevant mCRP that protects parental cancer cells from complement destruction, related to Figure 2. (A-C) The expression levels of CD59 (A), CD46 (B) and CD55 (C) were detected by FACS assays. (D and E) The levels of *CD59* mRNA (D) and protein (E) increased in the order of MCF-7, SK-BR-3, A549 and Calu-3 cells, as detected by qRT-PCR (D) or immunoblotting assays (E), respectively. (F) The order of parental cancer cell sensitivity to cetuximab-induced complement-meditated

destruction measured by CDC assays was highly correlated with CD59 levels (A). (G) CD59-insufficient parental cancer cells were more susceptible than CD59-sufficient parental cells to cetuximab-induced complement-meditated destruction. Data are represented as mean ± SD (n=3, independent experiments); ** $P<0.01$; and *** $P<0.001$. shSCR: scrambled shRNA; shCD59: specific shRNA against CD59.

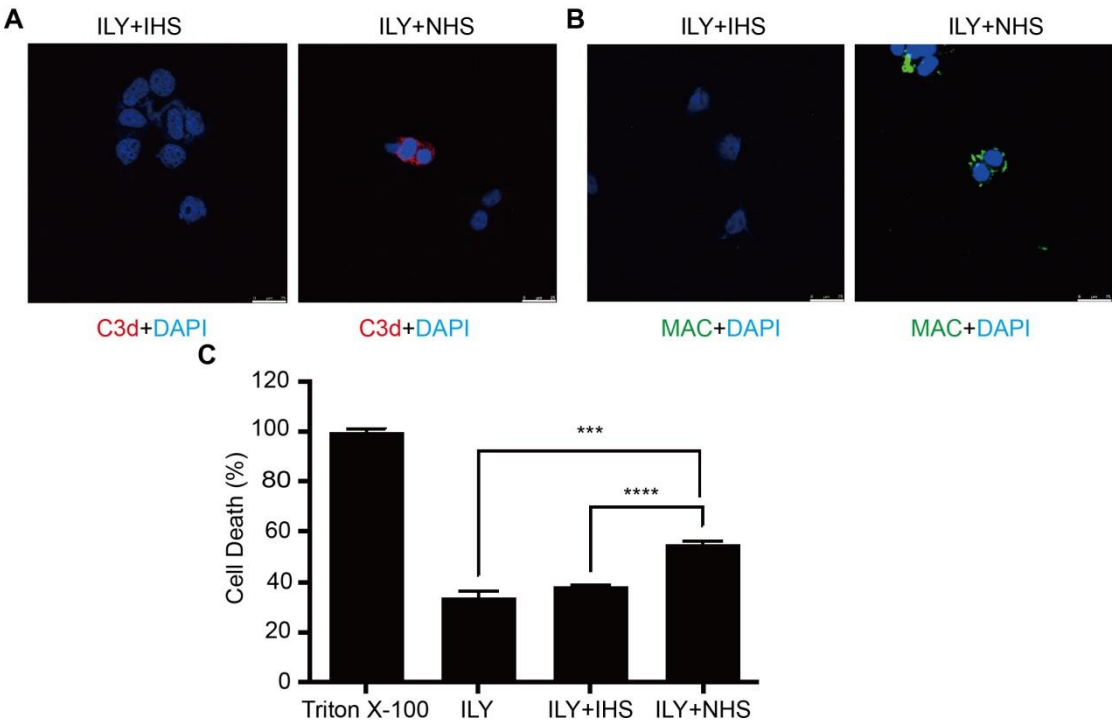

Figure S4. CD59-positive cell death induced by ILY treatment could activate complement in the survived CD59-negative MCF-7 parental cells, related to Figure 3. (A and B) ICC assay: C3d (A) and MAC (B) staining in ILY-treated cells with additional NHS or IHS administration. Scale bar represents 25 μm. (**C**) CDC assay: cell death induced by ILY treatment activated complement by NHS, leading to higher cell death rate than ILY alone and ILY plus HIS groups. Data are represented as mean ± SD (n=3, independent experiments); ***P<0.001; and ****P<0.0001. Triton X-100 induced total cell lysis as a positive control.

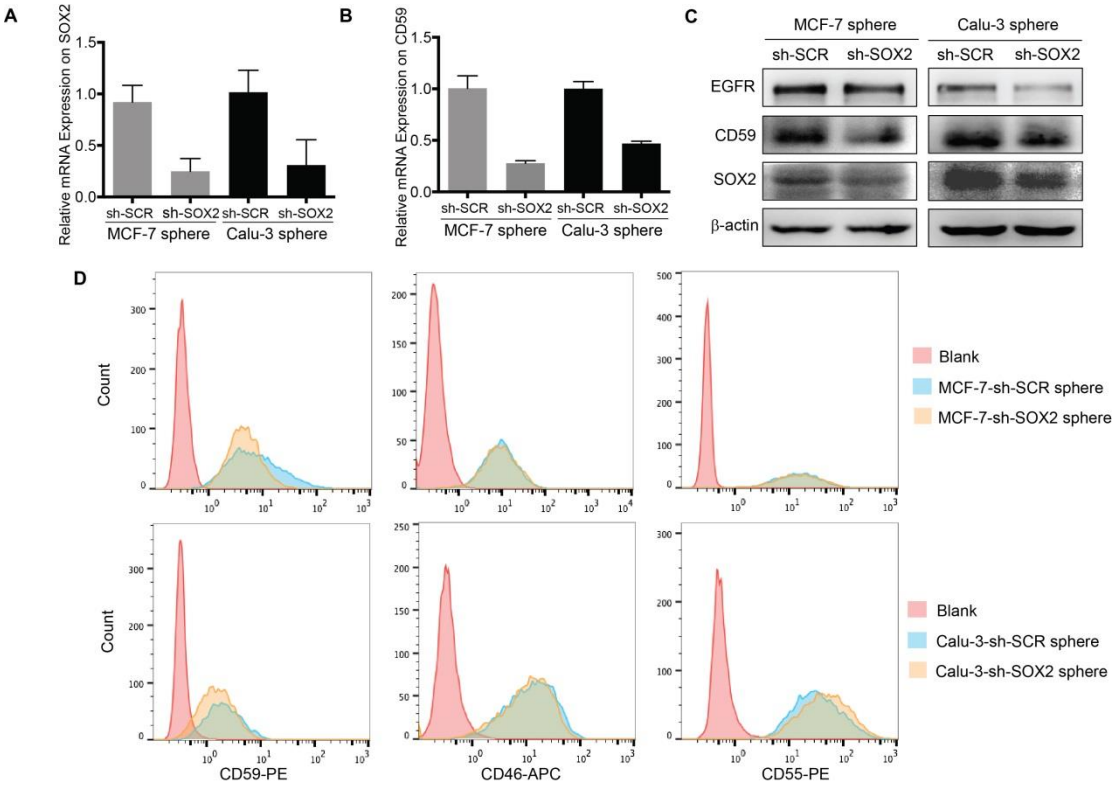

Figure S5. SOX2 insufficiency reduced the expression of CD59 in stem-like sphere forming cells, related to Figure 4. (A and B) SOX2 insufficiency (A) induced by specific shRNA reduced *CD59* transcription (B) in sphere forming cells. The mRNA levels of *SOX2* (A) and *CD59* (B) were measured by quantitative RT-PCR. Data are represented as mean ± SD (n=3, technical repeat). (C) Immunoblotting assay: The protein levels of EGFR, CD59 and SOX2 were remarkably reduced due to *SOX2* knocking-down in sphere forming cells. (D) FACS assay: The membrane level of CD59 but not of CD46 and CD55 was reduced by *SOX2* knocking-down.

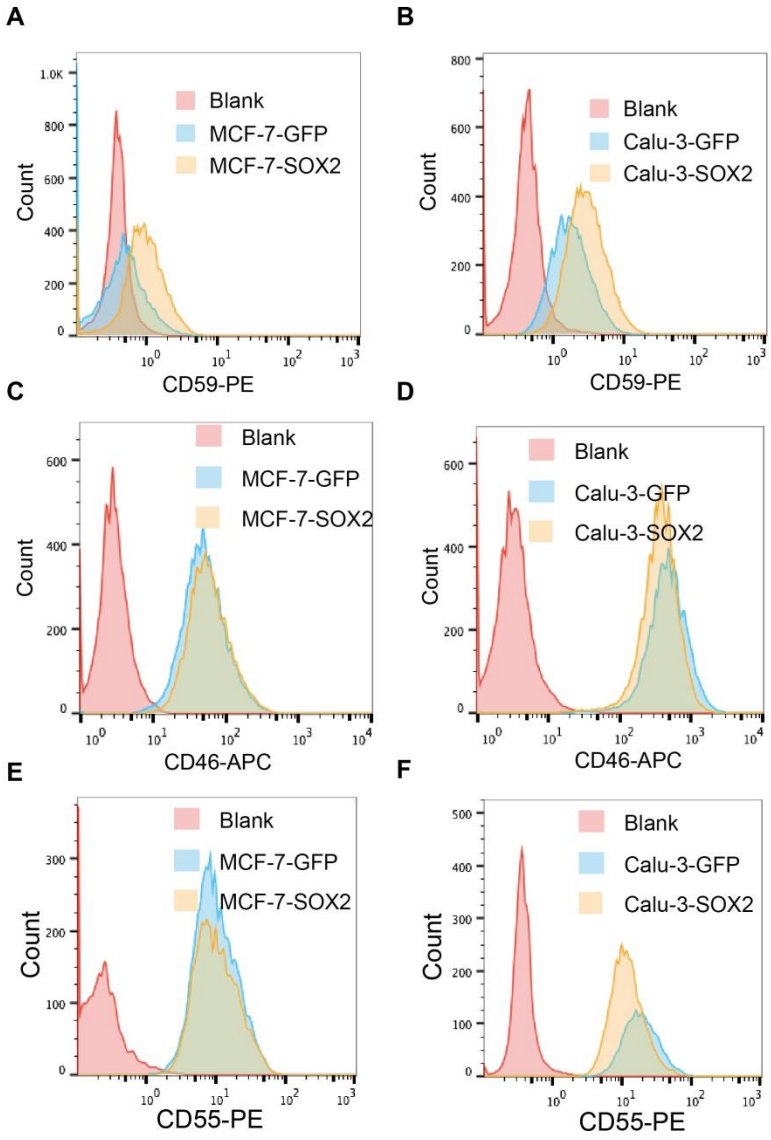

Figure S6. Ectopic SOX2 regulation effects on the expression of CD59, CD46 and CD55 in parental cells detected by FACS assay, related to Figure 5. (A and B) Ectopic SOX2 increased CD59 expression in MCF-7 (A) and Calu-3 (B) cells. (C-F) The CD46 (C and D) or CD55 (E and F) expression level was not increased by ectopic SOX2 in MCF-7 (C and E) or Calu-3 (D and F) cells, and ectopic SOX2 reduced the expression levels of CD46 (D) and CD55 (F) in Calu-3 cells.

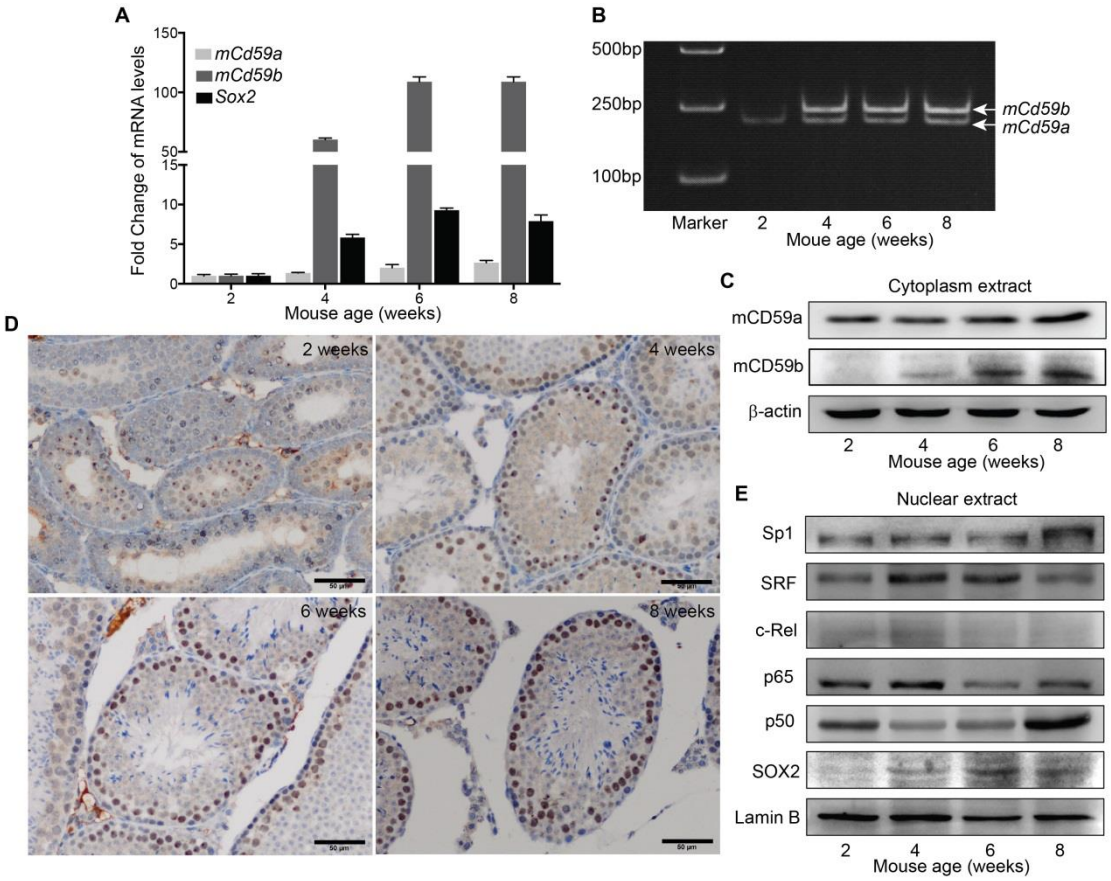

Figure S7. The expression of mCD59b but not of mCD59a is highly correlated with age with the level of SOX2 but not of other recognized transcription factors for *mCd59a* and *mCd59b* in mouse testis, related to Figure 6. Testis samples were collected from mouse with age of week 2, 4, 6 and 8. (A) Quantitative RT-PCR: the expression levels of *Sox2* and especially *mCd59b* but not of *mCd59a* were dramatically increased with age. Data were presented as mean ± SD, and experiments were biologically triplicated, n=3. (B) Reverse transcription PCR: a pair of primers that can amplify both *mCd59a* and *mCd59b* was employed, and PCR products (204 bp for *mCd59a*, and 237 bp for *mCd59b*) were separated by 5% PAGE. (C) Immunoblotting assay: cytoplasm level of mCD59b but not of mCD59a increased with age in mouse

testis samples. (D) SOX2 level increased with age detected by immunohistochemistry assay. Scale bar: 50 μm. (E) Immunoblotting assay: nuclear level of SOX2 but not of other recognized transcription factors for *mCd59a* and *mCd59b* increased with age in mouse testis.

Table S1. The commercial antibodies used in this study, related to methods.

Antibodies	Manufacturers	Applications in this study	Catalog Number
SOX2 (D6D9) XP Rabbit mAb	Cell Signaling Technology	WB (1:1,000), ChIP (5μg/test), IHC (1:100)	3579
Normal Rabbit IgG	Millipore	ChIP (5μg/test)	12-370
CD59 (H-7)	Santa Cruz Biotechnology	WB (1:500)	sc-133170
β-actin (C4)	Santa Cruz Biotechnology	WB (1:1,000)	sc-47778
NFKB p65 (F-6)	Santa Cruz Biotechnology	WB (1:500)	sc-8008
NFKB p50 (E-10)	Santa Cruz Biotechnology	WB (1:500)	sc-8414
c-Rel (B-6)	Santa Cruz Biotechnology	WB (1:500)	sc-6955
Lamin B (M-20)	Santa Cruz Biotechnology	WB (1:500)	sc-6217
Sp1 (E-3)	Santa Cruz Biotechnology	WB (1:500)	sc-17824
goat anti-mouse IgG-HRP	Santa Cruz Biotechnology	WB (1:10,000)	sc-2005
goat anti-rabbit IgG-HRP	Santa Cruz Biotechnology	WB (1:10,000)	sc-2004
EGF Receptor (D38B1) XP™ Rabbit mAb	Cell Signaling Technology	WB (1:1,000)	4267s
CREB-1 (24H4B)	Santa Cruz Biotechnology	WB (1:1,000)	sc-271
Anti-Smad3 (phosphoS423+S425) antibody (EP823Y)	abcam	WB (1:1,000)	ab52903
anti-Smad3 antibody	Arigo Biolaboratories	WB (1:500)	ARG53570
FITC Mouse Anti-Human CD59	BD Pharmingen	FACS (20μL/test)	555763
PE mouse Anti-Human CD59 (H19)	BD Pharmingen	FACS (20μL/test)	560953
PE anti-mouse/human CD44	BioLegend	FACS (5μL/test)	103007
PE anti-human CD46 (TRA-2-10)	BioLegend	FACS (5μL/test)	352401
FITC anti-human CD55 (JS11)	BioLegend	FACS (5μL/test)	311305
Hu CD55 PE (IA10)	BD Pharmingen	FACS (5μL/test)	561901

APC anti-human CD46 (TRA-2-10)	BioLegend	FACS (5μL/test)	352405
CD24-PerCP-Vio700	Miltenyi Biotec	FACS (10μL/test)	130-101-258
CD133/1 (AC133) -PE	Miltenyi Biotec	FACS (10μL/test)	130-098-826
Anti-C5b-9 antibody	abcam	IHC (1:200) ICC (1:100)	ab55811
Mouse Complement Component C3d Antibody	R&D SYSTEMS	IHC (1:200) ICC (1:100)	AF2655
p-CREB-1 (Ser133)	Santa Cruz Biotechnology	WB (1:500)	sc-101663
p300 (N-15)	Santa Cruz Biotechnology	WB (1:500)	sc-584
CBP (451)	Santa Cruz Biotechnology	WB (1:500)	sc-1211
SRF (D71A9) XP Rabbit mAb	Cell Signaling Technology	WB (1:1000)	5147
Alexa Fuor®488 goat anti-rabbit IgG (H+L)	Life Technologies	ICC (1:1000)	A-11034
Alexa Fuor®594 goat anti-mouse IgG (H+L)	Life Techonlogies	ICC (1:1000)	A-11005
peroxidase-conjugated affinipure goat anti-rabbit IgG H&L	Proteintech Group Inc.	IHC (1:200)	SA00001-2

Table S2. The sequences of primers and shRNA, related to methods.

Primers	5' to 3'
mouse *Sox2* CDS Forward primer	ATGTATAACATGATGGAGACGGAG
mouse *Sox2* CDS Reverse primer	TCACATGTGCGACAGGGGCA
human *SOX2* CDS Forward primer	ATGTACAACATGATGGAGACGGAG
human *SOX2* CDS Reverse primer	TCACATGTGTGAGAGGGG
human *SOX2* shRNA Forward primer	AATTAGGAGCACCCGGATTATAAATCTCGAGATTTATAATCCGGGTGCTCCTTTTTTTTAT
human *SOX2* shRNA Reverse primer	AAAAAAAAGGAGCACCCGGATTATAAATCTCGAGATTTATAATCCGGGTGCTCCT
CD59 shRNA Forward primer	CCGGGCTAACGTACTACTGCTGCAACTCGAGTTGCAGCAGTAGTACGTTAGCTTTTTG
CD59 shRNA Reverse primer	AATTCAAAAAGCTAACGTACTACTGCTGCAACTCGAGTTGCAGCAGTAGTACGTTAGC
scramble shRNA Forward primer	AATTCCTAAGGTTAAGTCGCCCTCGCTCGAGCGAGGGCGACTTAACCTTAGGTTTTTTT
scramble shRNA Reverse primer	AAAAAAACCTAAGGTTAAGTCGCCCTCGCTCGAGCGAGGGCGACTTAACCTTAGG
-2000 to -1 bp upstream *CD59* exon1 Forward primer	GAACATATAAGTGGAGATGTCCA
-2000 to -1 bp upstream *CD59* exon1 Reverse primer	GCCCCTCAGGATGCCCTT
-1000 to -1 bp upstream *CD59* exon1 Forward primer	TGGCCAGAGATAAACATGCAGT

-1000 to -1 bp upstream *CD59* exon1 Reverse primer	GCCCCTCAGGATGCCCTT
-350 to -1 bp upstream *mCd59b* exon1 Forward primer	GGGTTGAAAGAAGTAGAAGGAA
-350 to -1 bp upstream *mCd59b* exon1 Reverse primer	GGCTTAACATAACCCAGTGTTAG
human *CD59* qRT-PCR Forward primer	GCCAGTCTTTAGCACCAGTTG
human *CD59* qRT-PCR Reverse primer	TACACTTGTAACCCAGCTTTGG
human *CD59* ChIP Forward primer	AACAGTAGCTACCAGCTAAGTTGA
human *CD59* ChIP Reverse primer	AGACCCAAACAAAATGTTATGCGT
mCd59a qRT-PCR Forward primer	CTGACTCTAAGATTGCAGATTTGG
mCd59a qRT-PCR Reverse primer	TGAAGAAACCACCGGTTGGAA
mCd59b qRT-PCR Forward primer	TGTAGCCGGAAGGCAAGTGTATCA
mCd59b qRT-PCR Reverse primer	ACAAGTCCCACTGACAGCATTTGC
mCd59a/b reverse transcription PCR Forward primer	GATTCCTGTCTCTATGCTGTA
mCd59a/b reverse transcription PCR Reverse primer	CAAAATGGCCACCAGAAC

SI Materials and Methods

Cell culture and reagents

All cell lines in this study were purchased from the Type Culture Collection Cell Bank, Chinese Academy of Sciences. Mouse NIH/3T3 cells were maintained in Dulbecco's modified Eagle's medium supplemented with 10% fetal bovine serum and 1% penicillin/streptomycin. Human lung Calu-3 and cervical HeLa cancer cells were grown in Eagle's minimum essential medium supplemented with 10% fetal bovine serum and 1% penicillin/streptomycin, and human breast MCF-7 cancer cells were maintained in Eagle's minimum essential medium supplemented with human recombinant insulin (PeproTech, Rocky Hill, NJ) at a final concentration of 0.01 mg/ml, 10% fetal bovine serum and 1% penicillin/streptomycin. The human breast SK-BR-3 cancer cells were maintained in McCoy's 5a medium supplemented with 10% fetal bovine serum and 1% penicillin/streptomycin. The human lung A549 cancer cells were maintained in F-12K medium supplemented with 10% fetal bovine serum and 1% penicillin/streptomycin.

Normal human serum (NHS) as a complement resource was pooled from 10 healthy persons and aliquoted and then stored at −80°C until use. Heat-inactivated human serum (IHS) was prepared in a 65°C water bath for 30 min as a negative control. The anti-mCD59b polyclonal antibody was generated as previously described (Chen et al., 2015). Information regarding

the commercial antibodies used in this study is shown in Table S1.

Plasmid construction and lentiviral transduction

The coding DNA sequences (CDS) of human and mouse SOX2 were obtained by PCR amplification from cDNA pools of human A549 cells and mouse testis, respectively. These sequences were inserted into the pEGFP-N1 via EcoRI and BamHI endonuclease sites for transient SOX2 overexpression in HeLa or NIH/3T3 cells. The human SOX2 CDS was also cloned into the pCDH cDNA cloning and expression lentivector (Cat#CD511B-1, System Biosciences, Palo Alto, CA 94303) for stable SOX2 overexpression in MCF-7 or Calu-3 cells. The pLKO.1-TRC cloning vector (Plasmid #10878, Addgene, Cambridge, MA) was utilized to construct shRNA plasmids of scramble (SCR) and CD59-specific shRNA. The pLKO.3G cloning vector (Plasmid #14748, Addgene, Cambridge, MA) was used to construct shRNA plasmids of scramble (SCR) and SOX2-specific shRNA. The pCDH, pLKO.1 or pLKO.3G plasmid was co-transfected in 293FT cells with pMD.2G and psPAX2 plasmids to generate *SOX2* overexpression, *CD59* knock-down or *SOX2* knock-down lentivirus, respectively. The lentivirus was subsequently added to MCF-7 or Calu-3 culture medium with 8 μg/ml of polybrene (Sigma-Aldrich, USA) for 24 hours of incubation. The cells transfected with the CD59 knock-down lentivirus were selected using 5 μg/ml of puromycin (Sigma-Aldrich, USA), whereas the cells transfected with the *SOX2* overexpression or *SOX2* knock-down lentivirus

were sorted by GFP. Information regarding the primers for the SOX2 CDS cloning and RNAi targets is shown in Table S2.

Quantitative real-time PCR (qRT-PCR)

Total RNA from cells or mouse tissues was extracted with TRIzol reagent (Invitrogen, Grand Island, NY) and transcribed into cDNA using a Reverse Transcription System (Promega, Madison, WI). The input cDNA was standardized and then amplified for 40 cycles with SYBR Green Master Mix (Invitrogen, Grand Island, NY) and gene-specific primers on an ABI Prism 7900HT machine (Applied Biosystems, Waltham, MA). The *ACTB* gene encoding β-actin was used as an endogenous control, and the samples were analyzed in triplicate. The primers for qRT-PCR are listed in Table S2.

Reverse transcription PCR

The reverse transcription PCR was performed as previously described (Donev et al., 2008). In briefly, 200 ng of the cDNA from 2-, 4-, 6- and 8-week mouse testis were used as templates, respectively, and a pair of primers that can amplify both mCd59a and mCd59b was used in PCR for 22 cycles. The PCR products were separated in 5% poly-acrylamide gel, then the gel was scanned by ImageQuant RT ECL 350 (GE Healthcare, Little Chalfont, Buckinghamshire, UK). The primers for reverse transcription PCR are listed in Table S2.

Dual-luciferase reporter assay

We used a dual-luciferase reporter assay to identify the regions with promoter

activity in *mCd59b* and human *CD59* according to a previous report (Du et al., 2014). Various size fragments upstream of *mCd59b* and human *CD59* exon 1 were cloned and inserted into the pGL3 Basic Vector (Promega, Madison, WI); the primer sequences are shown in Table S2. Double-stranded DNA fragments with critical site mutations (see Figure 4C and Figure 6A) for SOX2 activity were synthesized by SBS Genetech Co., Ltd (Beijing, China). Then, the pGL3-derived plasmids together with the pRL-TK plasmid were co-transfected into HeLa or NIH/3T3 cells using Lipofectamine 2000 transfection reagent (Invitrogen, Grand Island, NY). After culturing for 48 hours, the dual-luciferase activities were measured using the dual-Luciferase Reporter Assay System (Promega, Madison, WI) on a Bio-Tek synergy HT microplate reader (Winooski, VT).

Chromatin immunoprecipitation (ChIP) assay

We performed ChIP assays as previously described (Du et al., 2014), and the related primers are shown in Table S2 and Figure 6A.

Immunoblotting assay

Immunoblotting assays were performed according to the standard protocol, and the related antibodies were shown in Table S1.

Fluorescence-activated cell sorting (FACS) analysis

Cells were detached using 0.25% trypsin/EDTA. After washing with PBS, the cells were incubated with fluorescein-conjugated antibodies for 30 minutes

and then washed and re-suspended in PBS. Flow cytometric analysis was performed with Cytomics FC 500 MPL (Beckman Coulter, Brea, CA) and analyzed with FlowJo software (Ashland, OR). Cell sorting was performed with a MoFlo XDP (Beckman Coulter, Brea, CA) according to the related fluorescence.

Immunohistochemistry (IHC) assay

For immunohistochemical staining, mouse tissue paraffin sections were incubated with 3% hydrogen peroxide to block endogenous peroxidase for 15 min at 37°C and rinsed in PBS, followed by high-pressure antigen retrieval in citrate buffer. Then, the sections were incubated with rabbit anti-SOX2 monoclonal antibody (1:100; Cell Signaling Technology, Danvers, MA) at 4°C overnight. After rinsing 3 times in PBS, the tissue sections were incubated with peroxidase-conjugated affinipure goat anti-rabbit IgG H&L (1:200; Proteintech, Chicago, IL) at room temperature for 1 hour. Then, the immunoreactivity was measured using a GTVision III immunohistochemical detection kit (GK500705; Gene Tech, Shanghai, China) according to the manufacturer's instructions.

Immunocytochemical (ICC) staining in intermedilysin (ILY)-treated cells

MCF-7 parental cells were treated by ILY (25 nM) for 2 hours, which could induced CD59-positive cell death rapidly via binding to CD59 (Hu et al., 2008). Further, the survived CD59-negative cells were added by NHS for complement activation or IHS as a negative control. CDC assay was used to determine the

cell death rate. ICC staining was used to detect C3d and MAC deposition in cell membrane according to the standard procedure, in which first antibodies against C3d or MAC, second antibody of Alexa Fuor®594 goat anti-mouse IgG (H+L) for C3d detection, and second antibody of Alexa Fuor®488 goat anti-rabbit IgG (H+L) for MAC detection were indicated in Table S1. The images were taken using a Leica TCS-SP5 confocal microscope.

Reference

Chen, J., Du, Y., Ding, P., Zhang, X., Zhang, L., Wang, N., and Hu, W. (2015). Mouse Cd59b but not Cd59a is upregulated to protect cells from complement attack in response to inflammatory stimulation. Genes and Immunity *16*, 437-445.

Donev, R.M., Sivasankar, B., Mizuno, M., and Morgan, B.P. (2008). The mouse complement regulator CD59b is significantly expressed only in testis and plays roles in sperm acrosome activation and motility. Mol Immunol 45, 534-542.

Du, Y., Teng, X., Wang, N., Zhang, X., Chen, J., Ding, P., Qiao, Q., Wang, Q., Zhang, L., Yang, C.*, et al.* (2014). NF-kappaB and enhancer-binding CREB protein scaffolded by CREB-binding protein (CBP)/p300 proteins regulate CD59 protein expression to protect cells from complement attack. J Biol Chem *289*, 2711-2724.

Hu, W., Ferris, S.P., Tweten, R.K., Wu, G., Radaeva, S., Gao, B., Bronson, R.T., Halperin, J.A., and Qin, X. (2008). Rapid conditional targeted ablation of cells expressing human CD59 in transgenic mice by intermedilysin. Nature medicine *14*, 98-103.